A MECHANISTIC AND A PROBABILISTIC MODEL FOR PREDICTING AND ANALYZING MICROBIOLOGICALLY INFLUENCED CORROSION

By

© Abdul-Waris Dawuda

A Thesis submitted to the

School of Graduate Studies

in partial fulfillment of the requirements for the degree of

Master of Engineering

Faculty of Engineering and Applied Science

Memorial University of Newfoundland

October 2019

St. John’s Newfoundland and Labrador.

Abstract

The complexities inherent in Microbiological Influenced Corrosion (MIC) requires a thorough understanding of the mechanisms involved when attempting to predict its rate. Even though mechanistic models have been developed in recent MIC studies, these models rarely analyze factors influencing pit depth and corrosion rate predicted. The objective of this work is to improve MIC prediction by quantitatively analyzing the factors influencing the predicted pit depth and corrosion rates. Therefore, this work presents a mechanistic and a probabilistic model which predicts corrosion rates, pit depth propagation, and analyzing influential factors in a MIC process. The mechanistic approach presents a model based on the direct contact extracellular electron transfer mechanism and nutrient limitation for microbial metabolism. The mechanistic model investigates the impact of redox intermediaries embedded in the cell structure of electroactive biofilms on corrosion rates. The mechanistic model also analyzes the effect of biofilm thickness limiting nutrient availability for corrosive microbiological organisms. The probabilistic approach presents a Bayesian network model which predicts the maximum corrosion rate in a process system. The probabilistic model analyzes the most critical factors affecting the corrosion rate predicted using Importance and Sensitivity analysis. The predictions obtained by both models were consistent with MIC rates in case studies and experimental studies. We also discovered that, redox properties of electroactive biofilms pose a significant threat to asset integrity as opposed to corrosion caused by sulfate reduction, in the case of Sulfate Reducing Bacteria (SRB).

Acknowledgment

I would like to express my profound gratitude to my supervisor Prof. Faisal Khan for giving me the opportunity to be part of this challenging and rewarding research project. He has been an exceptional source of guidance throughout the project and has contributed immensely to the success of this work. In addition, the invaluable input and guidance of the Memorial University Geno-MIC team have been a cornerstone to this research.

The Centre for Risk, Integrity, and Safety Engineering (C-RISE) association has been impactful in developing my networking and teamwork skills during my two-year study period. I thankfully acknowledge the financial support provided by Genome Canada through LSARP grant and Canada Research Chair (Tier I) in Offshore Safety and Risk Engineering.

Lastly, I would like to thank my parents, family, and friends for their constant support, prayers, and encouragement throughout my graduate school journey.

Table of Contents

List of Figures

List of Tables

List of Symbols, Nomenclature, and Abbreviations

E^{o}_{cell}	Cell Potential
E_{Fe}	Fe/Fe^{2+} potential
ΔH	Enthalpy
$i^{*}_{o,Fe}$	Anodic reference exchange current density
C_{H_2S}	Bulk H_2S concentration
C_S	Bulk SO_4^{2+} concentration
T_{ref}	Reference temperature
K_2	Langmuir adsorption model constant
E_S	Sulfate reduction reaction potential
C_Z	Cytochrome concentration
E_z	Cytochrome reduction reaction potential
k^0_z	Rate of electron transfer (biofilm/electrode)
L_B	length of the active transfer layer
D_S	SO_4^{2+} diffusivity constant
D_{H_2S}	H_2S diffusivity constant
R_i	Rate of reactions of diffusive species

$k_{f,Z}$	Forward reaction
$k_{b,Z}$	Backward reaction
F	Faraday constant
α	Coefficient of symmetry
R	Universal gas constant
T	Temperature
ΔG^{o}	Gibbs free energy
MIC	Microbiologically Influenced Corrosion
EET	Extracellular Electron Transfer
OM	Outer Membrane
SRB	Sulfate educing Bacteria
APB	Acid Producing Bacteria
IRB	Iron Reducing Bacteria
IOB	Iron Oxidizing Bacteria
EPS	Exopolymeric substances
BCSR	Biocatalytic Sulfate Reduction

Chapter 1

Introduction

Metals (e.g., aluminum, cast iron, carbon steel) processed from the ore have a persistent tendency to go back into its natural state. This phenomenon is known as oxidation in corrosion science [1]. Processed metals have significant economic value due to its properties such as ductility, malleability, luster, etc. The economic importance of processed metal is pervasive throughout the automotive, construction, manufacturing, and process industries. However, protecting these metallic materials from corrosion is a challenge because the infrastructure in oil and gas industries use alloys which have a high percent weight of iron, e.g., 97 wt.% Fe in X65 carbon steel, commonly used in pipelines [2].

Various corrosion types have been widely studied, but the effect of microorganisms on corrosion is still not well understood. Microorganisms are ubiquitous in our environment. These microorganisms are quite relevant in the food processing and mining industries [3]. However, microorganisms, directly and indirectly, contribute to material degradation and corrosion, thus posing as a threat to industrial safety and asset integrity. Microorganisms involved in corrosion is termed as Microbiologically Influenced Corrosion (MIC) [4-6].

Generally, corrosion, including MIC, plagues almost every industry, thereby making its economic impact profound. A lot of investments are made annually to curb corrosion and improve corrosion mitigation. In 2009, the city of Edmonton spent about $23.3 million (CAD) on emergency repairs of sewer systems due to acid corrosion caused by microorganisms [7]. U.S Federal Highway Administration (FHWA) reported a direct cost

of $276 billion in tackling corrosion between 1999-2002. This expense accounted for 6% of the U.S GDP within that period [8]. The NACE IMPACT report estimates global corrosion cost to be $2.5 trillion [10]. Additionally, MIC makes up 20% of most corrosion cases and accounts for 15-50% of corrosion costs [6, 8, 9, 11]. Globally, an estimated $14 trillion is spent on corrosion damages and mitigation measures [12].

Despite the economic implications, the limited understanding of MIC has stifled corrosion mitigation. The ability to predict MIC rates is invaluable to corrosion mitigation techniques. Hence, it is important to develop a mathematical model based on our current understanding of the processes that drive MIC and quantify corrosion rates. Because mechanistic models are formulated based on first principles, this makes them more reliable and widely applicable than other modeling techniques. However, assumptions are usually made in mechanistic models to simplify the modeling process; hence, some uncertainties are introduced into the model. Therefore, a probabilistic model is needed to cater for these uncertainties. Augmenting a mechanistic model with a probabilistic model also provides the flexibility for real-world application; hence, the goal of this thesis.

1.1 Research Objectives

The goal of this research is to develop a mechanistic and a probabilistic model to predict the corrosion rate influenced by microbiological organisms. In the mechanistic model, we shall investigate the effect of important biofilm properties such as biofilm conductivity and thickness on corrosion rates. Another objective of this work is to translate the mechanistic model into a probabilistic model. The goal of the probabilistic model is to provide

flexibility in incorporating additional factors into the model and analyze how important these factors are to the predicted corrosion rate. The objectives are summarized as follows:

- Develop a mechanistic model using electrochemical kinetics and Butler-Volmer principles.
- Investigate the effect of biofilm conductivity and thickness on corrosion rate and pit depth propagation.
- Translate the mechanistic model into a probabilistic model using a Bayesian network (BN).
- Update the probabilistic model with input factors not considered in the mechanistic model for better prediction and analysis of the input factors.

1.2 Thesis Structure

This thesis is a manuscript styled thesis which includes two submitted manuscripts. It is composed of five chapters. Chapter 1 provides an introduction which includes the implications of MIC, the features of some predictive models used in predicting corrosion, and the objectives of the thesis. Chapter 2 presents a literature review on MIC. The literature review focuses on the mechanisms and theoretical underpinnings of MIC. The review also discusses the predictive models developed in investigating corrosion rates of MIC. Chapter 3 is a manuscript that presents a mechanistic model is developed based on electrochemical kinetics and BV principles. The mechanistic model focuses on a nutrient controlled corrosion process. The model further investigates the effect of biological electron mediators that form part of a biofilm on corrosion rates. Lastly, the model also

considers the effect of biofilm thickness on corrosion. The manuscript is submitted to the International Journal of Corrosion Processes and Corrosion Control. Chapter 4 is a manuscript that presents a probabilistic model for predicting corrosion rate and analyzing how the factors prevalent in process industries impact the corrosion rate predicted. This manuscript is submitted to Corrosion Journal. Chapter 5 summarizes the outcomes of the thesis and recommendations on future research areas in MIC.

1.3 Novelty and contributions

Corrosion mechanistic models developed in literature can be argued as being empirical models because these models are calibrated using experimental data. This empirical approach is usually required when using the conventional corrosion modeling techniques, where experimental data is required for parameters like exchange current densities. However, these experimental data used in these models are obtained from controlled corrosion environments, hence reflect ideal conditions. In this work, we adopt by reverse engineering a framework developed in microbial fuel cell technology that is used to quantify current densities in electroactive biofilms. This approach is suitable because the basis of calculating corrosion rate depends on quantifying current densities of electron discharge from the anode. Secondly, this framework does not require exchange current density experimental data because it is a function of the redox property of the electroactive biofilm.

1.4 References

[1] P. Marcus, Corrosion mechanisms in theory and practice, CRC press, 2011.

[2] Y. Zheng, B. Brown, S. Nešić, Electrochemical study and modeling of H2S corrosion of mild steel, Corrosion. 70 (2013) 351-365.

[3] H. Flemming, P.S. Murthy, R. Venkatesan, K. Cooksey, Marine and industrial biofouling, Springer, 2009.

[4] R. Javaherdashti, Microbiologically influenced corrosion: an engineering insight, Springer, 2016.

[5] T.L. Skovhus, D. Enning, J.S. Lee, Microbiologically Influenced Corrosion in the Upstream Oil and Gas Industry, CRC Press, 2017.

[6] B.J. Little, J.S. Lee, Microbiologically influenced corrosion, John Wiley & Sons, 2007.

[7] L. Wu, C. Hu, W.V. Liu, The sustainability of concrete in sewer tunnel-A narrative review of acid corrosion in the city of Edmonton, Canada, Sustainability (Switzerland). 10, (2018).

[8] . S.P. Kotu, C. Erbay, N. Sobahi, A. Han, S. Mannan, A. Jayaraman, Integration of electrochemical impedance spectroscopy and microfluidics for investigating microbially

influenced corrosion using co-culture biofilms, NACE - International Corrosion Conference Series. 6 (2016) 4312-4325.

[9] . A.Y. Adesina, I.K. Aliyu, F. Al-Abbas, Microbiologically influenced corrosion (MIC) challenges in unconventional gas fields, NACE - International Corrosion Conference Series. 2015-January (2015).

[10] G. Koch, J. Varney, N. Thompson, O. Moghissi, M. Gould, J. Payer, International measures of prevention, application, and economics of corrosion technologies study, NACE International (2016).

[11] . L.L. Machuca, S.I. Bailey, R. Gubner, E. Watkin, A.H. Kaksonen, Microbiologically influenced corrosion of high resistance alloys in seawater, NACE - International Corrosion Conference Series (2011).

[12] Y. Li, D. Xu, C. Chen, X. Li, R. Jia, D. Zhang, W. Sand, F. Wang, T. Gu, Anaerobic microbiologically influenced corrosion mechanisms interpreted using bioenergetics and bioelectrochemistry: A review, Journal of Materials Science and Technology (2018).

Chapter 2

Literature Review

MIC is an interdisciplinary phenomenon broadly made of corrosion and microbiology. MIC studies in literature have been focused on the mechanisms involved in its process. Studying the mechanisms is required to understand, predict, and track the MIC process. In this section, we focus on the processes that lead to MIC, i.e., biofilm formation process. In addition, we discuss the bacteria groups commonly associated with MIC and their mechanisms. Lastly, we review the models in the existing literature that have been developed to predict and analyze MIC.

2.1 Biofilm formation and MIC

MIC is typically associated with areas where biofilms are present. A biofilm is a colony consists of different bacteria types that engage in processes that the individual microorganisms in that colony cannot independently engage in [1]. Therefore, a biofilm simply serves as a habitat for microorganisms. Biofilm formation is an important step in MIC because the synergistic relationship between the microorganisms allow them to metabolize, which in turn influences corrosion. Biofilms are formed due to the accumulation of immobilized microbiological cells that can grow and reproduce on a surface [1]. The process of biofilm growth on a surface is called biofouling [2]. During biofilm formation, extracellular polymers are secreted by the accumulated microorganisms. These extracellular polymers are called exopolymeric substances (EPS). EPS gives the biofilm its binding property, and inside the biofilm, it protects the

microorganisms from the environment [3]. Lewandowski [4], hypothesized that a biofilm enhances the survival of microorganisms and improves the transfer and availability of nutrients to the microorganisms. Another important role of EPS is that it controls the interfacial chemistry at the biofilm-metal interface, thereby making conditions such as pH and chemical species concentration at the interface radically different from the biofilm's external environment [1]. Figure 2.1 shows the evolution of a biofilm.

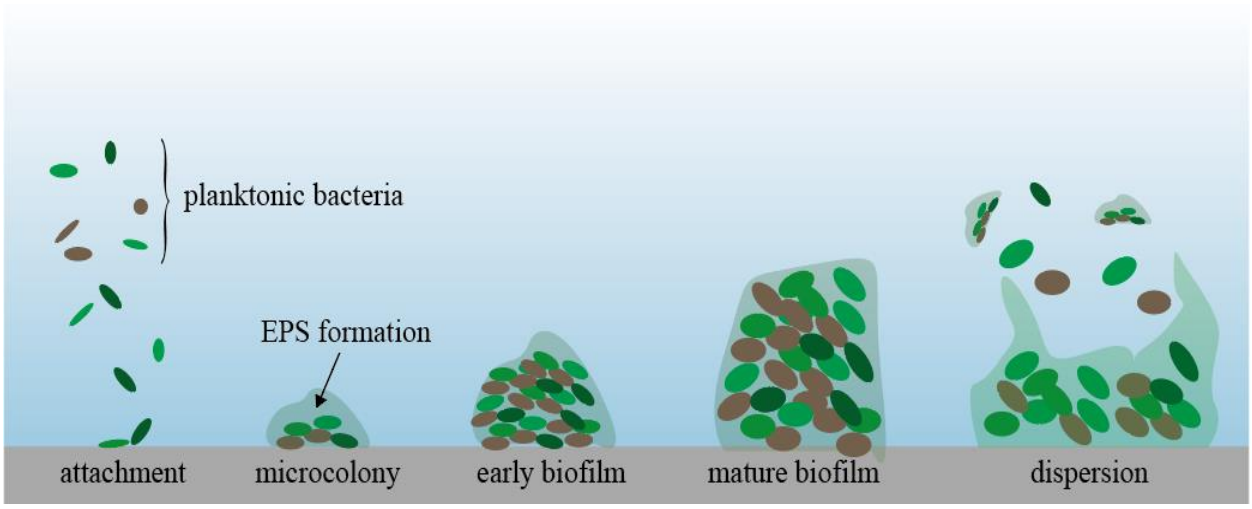

Figure 2.1 The evolution of biofilm formation [5]

Biofilm formation is influenced by so many conditions, and some key ones include; surface roughness/topography, surface wettability, and the presence of nutrients [6, 7]. Surface roughness is critical to the settlement of microbiological cells. In general, there is higher cell adhesion to rough surfaces, Korber et al. [8] proposed that rough surfaces tend to provide more surface area for microbiological cell adhesion. Sreekumari et al. [9] studied the impact of surface roughness on cell attachment by observing the attachment on welded surfaces on a 304L stainless steel compared to unwelded surfaces. Due to the roughness of

the welded surface, a significant microbiological cell attachment was observed as opposed to the unwelded surface.

The presence of a biofilm does not necessarily mean that MIC is present; however, it is a key observation when investigating MIC. All bacteria activities that cause MIC takes place within a biofilm. The bacteria activities within a biofilm colony that cause or promote MIC are referred to as the mechanisms. A good understanding of these mechanisms is necessary for a thorough MIC investigation. Because MIC is a type of corrosion, in the next section, we take a simple look at what corrosion is and how the microbiological activities influence corrosion on a metal surface.

2.2 Corrosion and MIC mechanisms

A refined metal/alloy has a lattice arrangement of elemental metal and electrons bonded tightly together. The metal elements are surrounded by a sea of electrons, known as a "Fermi Sea" [10]. A weak bond can cause the removal of electrons, which leads to the ionization of the elemental components of the metal, e.g., elemental iron, Fe^0 becomes Fe^{2+} when it loses electrons. This liberates the ionized elements into an aqueous solution/electrolyte, thereby causing the metal to corrode.

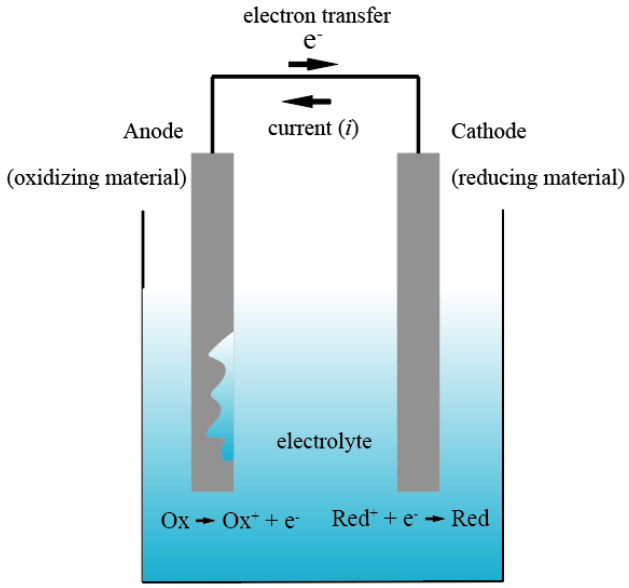

Figure 2.2 A corrosion model showing the oxidation reaction and metal loss in the anode and electron transfer to the cathode [11].

The basic principle of corrosion in metal is the loss of electrons from a metal to an electron acceptor, which causes the liberation of elemental metal ions. Interestingly, some microorganisms can utilize electrons from metal as an energy source during metabolism [1]. This electron utilization by bacteria is one major mechanism of MIC [12].

MIC is the process whereby the metabolic activities of microorganisms deteriorate a metal or a material [13]. Xu et al. [14] categorized MIC as Type I and Type II. Type I MIC is termed as electrogenic MIC (E-MIC) because it involves the bacteria directly taking up electrons from the metal surface. Typically, bacteria tend to take electrons from organic sources like lactate during metabolism. However, some bacteria type (e.g., lithotrophs) can take up electrons from the metal surface when an organic electron source is lacking [15,

16]. Aggressive pitting on sheets of pure iron (composition in wt.% : 99.877% Fe) have been reported by Venzlaff [17] and Xu et al. [14] when microbiological organisms turn to the metal surface as an electron source. This type of MIC is only peculiar to electroactive bacteria, and their conductive mechanism is still an active research area regarding the role of microbiological organisms in corrosion.

Type II MIC, on the other hand, occurs when the metabolic end products of bacteria become electron acceptors. Type II MIC is sometimes called chemical MIC (C-MIC) or Metabolite MIC (M-MIC) [14, 18]. Type II MIC is peculiar to fermentative bacteria like Acid Producing Bacteria (APB).

Different types of bacteria are involved in a MIC process. The common bacteria types include [5, 19];

- Sulfate Reducing Bacteria (SRB)/ Sulfate Reducing Prokaryotes (SRP)
- Methanogens,
- Acid Producing Bacteria (APB),
- Iron Oxidizing and Reducing Bacteria (IOB and IRB, respectively).

All these bacteria types have a unique way of contributing to MIC. However, they all fall under either Type I or Type II MIC. The mechanisms of MIC can be broadly categorized as;

- Concentration cells
- Microbial activities producing corrosive metabolites
- The synergy of bacteria in complex biofilm consortia accelerating corrosion

2.2.1 Concentration cells

A biofilm deposit on metal in an environment where dissolved oxygen concentration is high can induce anodic and cathodic zones on the metal surface. Surfaces underneath a thick biofilm may lack oxygen because of the oxygen concentration gradient across the biofilm. The oxygen concentration gradient can be caused by respiring aerobic bacteria, thereby leaving the metal surface underneath the biofilm with less oxygen compared to the adjacent surface with no biofilm deposit. If pitting has been initiated under the biofilm deposit, this will create a cathodic zone at the bare metal surface with high oxygen concentration close to the pit underneath the biofilm. Because oxygen can accept electrons, the anodic dissolution causing pit formation under the biofilm will allow electrons to accumulate at the surfaces where oxygen concentration is high. This mechanism is also described as differential aeration cells [5].

2.2.2 Microbial activities producing corrosive metabolites

Metabolic by-products from some microorganisms can attack the metal surface. SRB metabolism produces biotic H_2S, which is a highly corrosive substance. Biotic H_2S can react with carbon steel to produce corrosion products of the form Fe_xS_y (e.g., mackinawite) [7]. These deposits formed can contribute to the formation of differential aeration cells on the metal surface, which induces further corrosion. In an aerobic environment, the reaction of Fe_xS_y with oxygen can produce corrosive elemental sulfur (S^0) [5, 7]. Acetic acid produced by APB is another important corrosive metabolic by-product. Acetic acid can be directly reduced with electrons from the metal surface or by dissociating to produce protons

(H^+) which can cause a low pH within the biofilm, thus making the surface beneath the deposit susceptible to corrosion [12, 18].

2.2.3 Synergy of bacteria in complex biofilm consortia accelerating corrosion

A bacteria's metabolic by-products can be a nutrient requirement for another bacteria's metabolism. The synergy between bacteria in a biofilm is important for biodiversity. Biotic H_2S from SRB can produce H^+ when it dissociates. H^+ is subsequently reduced by electrons from the metal surface to form H_2, which is a direct requirement for Methanogens during metabolism. Some bacteria types with conductive structures like nanowires or pilis can shuttle electrons into the biofilm consortium which can then be utilized by bacteria inside the biofilm. This conductive property of bacteria is demonstrated by Enning et al. [20], whose experiment cultured SRB within a system where the only one electron donor was present and with CO_2 as the only carbon source. The result of the experiment showed aggressive pitting and "intimate SRB growth" on the metal surface.

Considering how these corrosive bacteria types cause corrosion, identifying them is critical in MIC forensics because it can provide insight into how MIC is occurring. Currently, microbiological molecular methods (MMM) such as polymerase chain reaction (PCR) and quantitative polymerase chain reaction (qPCR) analysis are the techniques used to identify active bacteria in a MIC environment [21-23]. Even though identifying the bacteria is an important step in MIC forensics, it cannot predict the corrosion rate. Therefore, attempts have been made to develop models to predict MIC rates.

2.3 State of the art in MIC predictive models

Peng et al. [24] developed a mechanistic model to predict corrosion rate based on SRB growth kinetics. The model assumed a biofilm to be in an existing pit, where the corrosion rate is proportional to the rate of nutrient/substrate (sulfate) consumption. The model assumes sulfate to be the only growth-limiting substrate for SRB. The transport equation is used to model the diffusion of sulfate to the SRB in the pit. The model assumes that the rate of sulfate flux into the biofilm is equal to the rate of sulfate consumption by SRB. Hence, the Monod equation is used to describe the rate of nutrient utilization in SRB growth kinetics. Because of the interfacial process of corrosion, the model considers sulfate consumption as a boundary condition at the metal biofilm interface. Sulfate concentration is also considered to be constant in the bulk fluid. Peng et al. [24] adopted the cathodic SRB mediated depolarization theory to describe the electron consumption process by SRB. This cathodic SRB mediated depolarization theory considers the consumption of adsorbed hydrogen (H_{ad}) instead of H_2 proposed by the cathodic depolarization theory (CDT) by Wolgozen Kuhr and Van der Vlugt. The cathodic SRB mediated depolarization is chemically described as [25];

Anodic reaction: $4Fe \rightarrow 4Fe^{2+} + 8e^{-}$ (2.1)

Water dissociation: $8H_2O \rightarrow 8H^{+} + 8OH^{-}$ (2.2)

Cathodic reaction: $8H^{+} + 8e^{-} \rightarrow 8H_{ad}$ (2.3)

Cathodic SRB depolarization: $SO_4^{2-} + 8H_{ad} \rightarrow S^{2-} + 4H_2O$ (2.4)

Corrosion products: $Fe^{2+} + S^{2-} \rightarrow FeS$ (2.5)

$$3Fe^{2+} + 6OH^- \rightarrow 3Fe(OH)_2 \quad (2.6)$$

Overall balanced reaction: $4Fe + SO_4^{2-} + 4H_2O \rightarrow FeS + 3Fe(OH)_2 + 2OH^-$ (2.7)

Al Darbi et al. [26] also developed a similar mechanistic model as Peng et al. [24], with similar assumptions of a biofilm in a pit. Their model, however, considers a sink reaction in the transport equation, representing the consumption of sulfate within the diffusion profile. These models focus on the mechanism of SRB metabolism causing MIC, hence nutrient available to SRB is considered a limiting factor. However, the models are only limited to SRB and do not consider how bacteria consumes electrons from metals.

Gu [27] developed a mechanistic model based on the biocatalytic sulfate reduction (BCSR) theory. Gu [27] approach focuses on the electrochemical kinetics of anodic and cathodic reactions, hence the application of Butler-Volmer equations. The BCSR theory proposes that a bacterium consumes electrons from the metal for sulfate reduction. And this sulfate reduction reaction occurs in the cytoplasm of the bacterium [12, 18].

Anodic reaction: $Fe \rightarrow Fe^{2+} + 2e^-$ (2.8)

The cathodic reaction: $SO_4^{2-}+8H^+ + 8e^- \rightarrow HS^-+OH^-+3H_2O$ (2.9)

H_2S production by SRB: $HS^- + H^+ \rightarrow H_2S$ (2.10)

Therefore, current densities generated due to the transfer of electrons from the metal to the biofilm are quantified with the Butler-Volmer equations. The model also accounts for the mass transfer of sulfate to the sessile bacteria attached to the metal. Hence both mass and charge transfer resistance are considered limiting factors in the model. Xu et al. [14]

adopted Gu [27] model by including Acid Producing bacteria. Acetic acid produced by APB is considered a cathodic reaction in addition to sulfate reduction by SRB.

Acetic acid reduction: $2HAc + 2e^- \rightarrow 2Ac^- + H_2$ (2.11)

Both models, however, do not incorporate bacteria growth kinetics; also, the models can be considered semi-empirical because some electrochemical data used were generated from experiments. The corrosion rate for both models is calculated directly by using the anodic current density because it quantifies the rate at which electrons are lost from the metal surface. The corrosion rate equation is given as [28];

Corrosion rate $CR\left(\frac{mm}{yr}\right) = \frac{MW_{Fe}}{2F\rho_{Fe}} i_{Fe}$ (2.12)

Where;

MW_{Fe} = Molecular weight of Fe (kg/mol)

ρ_{Fe} = Density of Fe (kg/m^3)

i_{Fe} = Current density for anodic reaction (A/m^2)

2.4 Extracellular Electron Transfer (EET) mechanism

The emergence of microbial fuel cell (MFC) technology has improved the understanding of the electron transfer process between biofilms and metals [29]. A biofilm with a conductive property is called an electroactive biofilm [30]. Because corrosion involves the transfer of electrons from the metal to an electron acceptor, MIC can be well described with the concept of electron transfer from a metal to an electroactive biofilm. This idea is

supported by the BCSR theory, which proposes that electrons from a metal surface are consumed by a colony of bacteria attached to it. Electrons sources for bacteria metabolism include; 1) Organic carbon source and 2) Metal surface. In MIC, some bacteria types directly consume electrons from an external source (Metal) in the absence of an organic carbon source. This is known as extracellular electron transfer (EET) [31].

The three distinct EET mechanisms proposed by researchers include [31]: 1) the direct electron transfer between bacteria and the electron source or the electron carriers. 2) soluble electron shuttle (i.e., a compound that carries electrons) transporting electrons from the metal surface to the bacteria that is not in contact with the metal; and 3) conductive extracellular components of the bacteria or biofilm matrix, anchored onto the metal surface.

Korth et al. [30] developed a framework for modeling the electron transfer process under the direct contact EET mechanism between metal and biofilm. The framework enables the quantification of the exchange current density of the cathodic and anodic reaction processes without resorting to experimental data. Renslow et al. [32] also developed a framework in modeling the electron transfer process in an electroactive biofilm. The framework considers two key EET mechanisms, which include the diffusion-based and the conduction-based electron transfer mechanism. Even though both frameworks present models that describe electrons transfer from the biofilm to the metal surface (i.e., bioanodes), the electron transfer process is reversible, and the reverse is MIC. In MIC, the biofilm becomes a biocathode, and the electron transfer process from metal to biofilm has been established experimentally by Venzlaff et al. [17] and Xu et al. [33].

2.5 Conclusion and knowledge gaps

The frameworks developed for EET mechanisms can be used to calculate parameters such as cathodic exchange current densities in mechanistic models. However, none of the models explicitly adopt one of the EET mechanisms in modeling the cathodic exchange current density needed to calculate the corrosion rate. Therefore Gu [18, 27], Xu [14], Peng et al. [24] and Al-Darbi [26] models are calibrated using exchange current densities from experimental data, thus can be argued as semi-empirical models. In addition, these modeling approach used in predicting MIC is not practical because it only gives corrosion rate trends in conditions that do not reflect real conditions. A predictive model should be able to analyze conditions and factors contributing to the corrosion rate predicted. With MIC being a complex process, it means a wide range of factors is critical to its progress. Chapter 3 of this thesis presents a mechanistic model to predict MIC rates and the effect of biofilm growth on corrosion rates. This mechanistic model is based on an EET framework. Chapter 4 of this thesis presents a probabilistic model whose objective is to analyze contributing effects on a predicted MIC rate. Thus, this probabilistic model expounds on factors critical to MIC rates.

2.6 References

[1] B.J. Little, J.S. Lee, Microbiologically influenced corrosion, John Wiley & Sons, 2007.

[2] H. Flemming, P.S. Murthy, R. Venkatesan, K. Cooksey, Marine and industrial biofouling, Springer, 2009.

[3] I.B. Beech, J. Sunner, Biocorrosion: Towards understanding interactions between biofilms and metals, Curr. Opin. Biotechnol. 15 (2004) 181-186.

[4] . Z. Lewandowski, Structure, and function of bacterial biofilms (1998).

[5] T.L. Skovhus, D. Enning, J.S. Lee, Microbiologically Influenced Corrosion in the Upstream Oil and Gas Industry, CRC Press, 2017.

[6] M. Taleb-Berrouane, F. Khan, K. Hawboldt, R. Eckert, T.L. Skovhus, Model for microbiologically influenced corrosion potential assessment for the oil and gas industry, Corrosion Engineering, Science and Technology (2018) 1-15.

[7] A. Ibrahim, K. Hawboldt, C. Bottaro, F. Khan, Review and analysis of microbiologically influenced corrosion: the chemical environment in oil and gas facilities, Corrosion Engineering, Science, and Technology. 53 (2018) 549-563.

[8] D. Korber, A. Choi, G. Wolfaardt, S. Ingham, D. Caldwell, Substratum topography influences susceptibility of Salmonella enteritidis biofilms to trisodium phosphate., Appl. Environ. Microbiol. 63 (1997) 3352-3358.

[9] K.R. Sreekumari, K. Nandakumar, Y. Kikuchi, Bacterial attachment to stainless steel welds: Significance of substratum microstructure, Biofouling. 17 (2001) 303-316.

[10] E. McCafferty, Introduction to corrosion science, Springer Science & Business Media, 2010.

[11] R.W. Revie, Corrosion, and corrosion control: an introduction to corrosion science and engineering, John Wiley & Sons, 2008.

[12] T. Gu, D. Xu, Demystifying MIC mechanisms, CORROSION 2010 (2010).

[13] T. Liengen, R. Basseguy, D. Feron, I. Beech, V. Birrien, Understanding biocorrosion: fundamentals and applications, Elsevier, 2014.

[14] D. Xu, Y. Li, T. Gu, Mechanistic modeling of biocorrosion caused by biofilms of sulfate reducing bacteria and acid producing bacteria, Bioelectrochemistry. 110 (2016) 52-58.

[15] B.J. Little, J.S. Lee, R.I. Ray, The influence of marine biofilms on corrosion: a concise review, Electrochim. Acta. 54 (2008) 2-7.

[16] K. Fischer, Mathematical modelling of electron transfer modes in electroactive microorganisms (2017).

[17] H. Venzlaff, D. Enning, J. Srinivasan, K.J.J. Mayrhofer, A.W. Hassel, F. Widdel, M. Stratmann, Accelerated cathodic reaction in microbial corrosion of iron due to direct electron uptake by sulfate-reducing bacteria, Corros. Sci. 66 (2013) 88-96.

[18] . T. Gu, Can acid producing bacteria be responsible for very fast MIC pitting? NACE - International Corrosion Conference Series. 2 (2012) 1481-1493.

[19] R. Javaherdashti, Microbiologically influenced corrosion: an engineering insight, Springer, 2016.

[20] D. Enning, H. Venzlaff, J. Garrelfs, H.T. Dinh, V. Meyer, K. Mayrhofer, A.W. Hassel, M. Stratmann, F. Widdel, Marine sulfate-reducing bacteria cause serious corrosion of iron under electroconductive biogenic mineral crust, Environ. Microbiol. 14 (2012) 1772-1787.

[21] . C. Baird, D. Ogles, B.R. Baldwin, Molecular microbiological methods to investigate microbial influenced corrosion in fully integrated kraft pulp and paper mills, NACE - International Corrosion Conference Series. 2 (2016) 1293-1303.

[22] . R. Sooknah, S. Papavinasam, R.W. Revie, Monitoring microbiologically influenced corrosion: A review of techniques, NACE - International Corrosion Conference Series (2007) 075171-0751717.

[23] . U.S. Thomsen, R.L.C. Meng, J. Larsen, Monitoring and risk assessment of microbiologically influenced corrosion in offshore pipelines, NACE - International Corrosion Conference Series. 1 (2016) 766-778.

[24] C. Peng, S. Suen, J. Park, Modeling of anaerobic corrosion influenced by sulfate-reducing bacteria, Water Environ. Res. 66 (1994) 707-715.

[25] A. Marciales, Y. Peralta, T. Haile, T. Crosby, J. Wolodko, Mechanistic Microbiologically Influenced Corrosion Modeling—A Review, Corros. Sci. (2018).

[26] M. Al-Darbi, K. Agha, M. Islam, Comprehensive modelling of the pitting biocorrosion of steel, The Canadian Journal of Chemical Engineering. 83 (2005) 872-881.

[27] . T. Gu, K. Zhao, S. Nesic, A new mechanistic model for mic based on a biocatalytic cathodic sulfate reduction theory, NACE - International Corrosion Conference Series (2009).

[28] T. Gu, Theoretical Modeling of the Possibility of Acid Producing Bacteria Causing Fast Pitting Biocorrosion, Journal of Microbial and Biochemical Technology. 6 (2014) 68-74.

[29] L. Huang, J.M. Regan, X. Quan, Electron transfer mechanisms, new applications, and performance of biocathode microbial fuel cells, Bioresour. Technol. 102 (2011) 316-323.

[30] B. Korth, L.F. Rosa, F. Harnisch, C. Picioreanu, A framework for modeling electroactive microbial biofilms performing direct electron transfer, Bioelectrochemistry. 106 (2015) 194-206.

[31] C.I. Torres, A.K. Marcus, H. Lee, P. Parameswaran, R. Krajmalnik-Brown, B.E. Rittmann, A kinetic perspective on extracellular electron transfer by anode-respiring bacteria, FEMS Microbiol. Rev. 34 (2010) 3-17.

[32] R. Renslow, J. Babauta, A. Kuprat, J. Schenk, C. Ivory, J. Fredrickson, H. Beyenal, Modeling biofilms with dual extracellular electron transfer mechanisms, Physical Chemistry Chemical Physics. 15 (2013) 19262-19283.

[33] D. Xu, Y. Li, F. Song, T. Gu, Laboratory investigation of microbiologically influenced corrosion of C1018 carbon steel by nitrate reducing bacterium Bacillus licheniformis, Corros. Sci. 77 (2013) 385-390.

Chapter 3

Mechanistic modeling of MIC considering Sulfate reduction and Direct Contact Extracellular Electron Transfer (EET)

Preface

This manuscript has been submitted to the Journal of Materials Science and Technology and currently under review. I am the first author of this manuscript, and Dr. Faisal Khan is the corresponding author. Other co-authors include Dr. Kelly Hawboldt and Dr. Ibrahim Adeoti. I developed the mechanistic model, implemented the model using data from literature, and tested the model's results against existing results from microbial corrosion experiments. Dr. Faisal Khan reviewed the model, its results, and provided constructive feedback which was crucial to the improvement of the model. Dr. Kelly Hawboldt and Dr. Ibrahim Adeoti reviewed and suggested improvements on the chemical reactions and the chemistry involved in the corrosion process. The feedback and suggestions from the co-authors were vital in the development of the final draft of the manuscript.

Abstract

New insights on the extracellular electron transfer (EET) between electroactive biofilm and metals have improved the understanding of Microbiological Influenced Corrosion (MIC). The Biocatalytic Sulfate Reduction theory hypothesizes the transfer of electrons from metal into the cytoplasm of sessile sulfate-reducing bacteria (SRB) for SRB metabolism. However, the well-established EET mechanisms in literature are rarely adopted in modeling this electron transfer process in MIC mechanistic models. In this work, a

mechanistic model is developed to predict the corrosion rate using one of the EET mechanisms known as the direct contact EET. Results of the model are compared with laboratory corrosion rate data and observed a consistent behavior. Maximum corrosion rates of 0.55mm/yr. and 0.98mm/yr. were recorded for an SRB biofilm thickness of 20 and 5 microns, respectively. The study also investigates the impact of electron mediators as electron carriers and shows that electron mediators have important implications in MIC.

3.1 Introduction

Much progress has been made in the understanding of Microbiological Influenced Corrosion (MIC) in terms of developing mechanistic models to predict corrosion rates [1-3]. Predictive models are vital in preventing the impacts of MIC [4, 5] as it is estimated to make up 20% of all corrosion cases and about 15-50% of corrosion costs [6-8]. The United States (U.S) and Australia spend about $1.3 billion [6] and $5 billion, respectively, on corrosion annually [9]. Developments in microbial extracellular electron transfer (EET) has improved the understanding of the mechanisms involved in MIC [10-13]. Frameworks and techniques have been developed to model the EET mechanisms [11, 12]. However, these techniques are rarely adopted in MIC mechanistic models.

MIC is a type of corrosion which deteriorates a material due to microbial “metabolic activities” [7, 14]. And EET describes the relationship between electron transfer and microbial metabolism [12, 15].

Microbes can generally cause corrosion by; Producing corrosive metabolic products; Consuming electrons from metals during metabolism; Creating deposits that form

differential aeration cells; Removing passivation layers; and Consuming corrosion inhibiting chemical species [16-18].

The electron consumption mechanism for metabolism by microbes have shown rapid material deterioration within short periods [19], and this mechanism is consistent with the concept of EET [10, 15].

So far, three EET mechanisms have been proposed to describe electron transfer between metal and biofilm. They include [15]; Soluble electron shuttle; Direct contact; and Solid conductive components or matrix (pili or nanowires) in a biofilm.

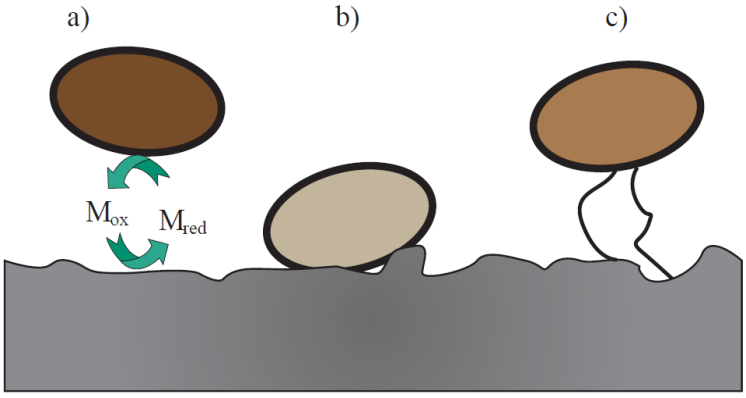

Figure 3.1 The three EET mechanism by electroactive microbial cells [15]: a) soluble electron shuttle b) direct contact; and c) solid conductive matrix.

Figure 3.1 is adopted and modified from an anode respiring bacteria, in that, we alter the direction of the electron transfer process where electrons are moving from the metal into the bacteria. In Figure 3.1a, the soluble mediator is shuttling electrons to the bacteria from the metal in its reduced form.

All three mechanisms in Figure 3.1 can coincide in a biofilm-metal environment [20]. The soluble electron shuttle mechanism proposes that a chemical compound with a redox property can transport electrons between metal and biofilm by diffusion. In the case of MIC, a bacterium that is not close to the metal can still have access to electrons via diffusive transport of reduced soluble shuttles [21, 22].

Direct contact mechanism requires the bacterium or microbial cell to be in contact with the metal surface [23, 24]. This mechanism does not require an electron shuttle, but rather a "promoter," which is a compound that binds the cell to the metal surface [25]. This binding facilitates electron transfer through the redox property of the protein-membrane embedded in the bacterium's cell wall [15]. However, the "promoter" does not take part in the electrochemical process [25].

The solid conductive matrix mechanism is like the direct contact mechanism, but the bacterium or microbial cell need not be in contact with the metal [26]. Here, electrons are transported through a conductive matrix known as pili or nanowires that are anchored to the metal surface [27, 28]. It has been reported that cytochromes form part of these nanowires, thus giving it a conductive property [29, 30].

These EET mechanisms have been used to develop frameworks to quantify current densities generated from electron transfer between metal and biofilm [11, 12, 28, 30]. EET techniques have been used in other domains [11, 12], and applied in describing MIC mechanisms [31, 32]. Even though EET has been well studied in anode respiring bacteria, where electrons are transferred from the bacteria to the metal to harness electrical energy

for MFCs, electron transfer between metal and biofilm is reversible because biological cathodes have also been used in microbiological fuel cells. A biological cathode includes microorganisms that accept electrons from the anode. And this electron transfer mechanism (i.e., from the metal into the bacteria) correlates with one of the major MIC mechanisms, which is the electron consumption mechanism by bacteria. [13, 15]. This mechanism is thoroughly explained under MIC and direct contact EET mechanism section.

Hence, the objective of this work is to; Develop a mechanistic model to predict corrosion rate; Use the direct contact EET mechanism to describe the kinetics of electron transfer from a metal to an electroactive and anaerobic Sulfate Reducing Bacteria (SRB) biofilm.

The subsequent sections of this manuscript include; section 3.2, which describes the theory behind electron consumption mechanism of bacteria and the direct contact mechanism. Section 3.3, which focuses on the mechanistic model development, section 3.4, briefly describes the methodology, shows the results of simulations and discussion. Section 3.5 concludes our findings.

3.2 MIC and Direct Contact Extracellular Electron transfer (EET) Mechanism

MIC is an electrochemical and a biological process [33, 34] that is common in anaerobic environments where SRB are active [34, 35]. SRB and many other bacteria types consume electrons as an energy source to facilitate catabolic reactions during metabolism [36]. Electrons may come from either organic carbon sources or the metal [14, 37]. MIC occurs when electrons come from the metal [38].

In 1934, Von Wolzogen Kuhr and Van der Vlugt proposed the Cathodic Depolarization Theory (CDT) to explain MIC based on the electron consumption mechanism [17]. The CDT proposes that in anoxic conditions, hydrogen ion (H^+) is an "electron carrier" when reduced to molecular hydrogen (H_2) [13]. Molecular hydrogen H_2 is then consumed by hydrogenase-SRB to catalyze sulfate reduction during metabolism [39]. CDT implies an electron transfer from metal to bacteria via molecular hydrogen [40], thus causing MIC; however, some bacteria such as hydrogenase-negative SRB can consume electrons via different "carriers" otherwise known as "mediators" or "redox intermediaries" [41]. This disparity, among others, led to the proposal of other mechanisms of MIC in terms of electron transfer [17] including the Biocatalytic Sulfate Reduction (BCSR) theory by Gu [1].

The BCSR theory proposes a far more complex MIC mechanism; nonetheless, it implies a biological cathode, where sulfate is reduced in the cytoplasm of a bacterium [2]. The BCSR theory does not explicitly state which EET mechanism governs the electron transfer process between bacteria and metal because all three EET mechanisms described earlier can co-occur. Therefore, this work focuses on the direct contact EET mechanism which proposes that a bacterium (SRB) in contact with a metal surface consumes electrons by transferring them across its cell wall [13, 23], where this electron transfer can be achieved through a chain of redox reactions via protein membranes in its cell wall called cytochromes (c-type) [15].

Cytochromes (c-type) are protein membranes embedded in the cell wall of some SRB, e.g., *Disulfovibrio vulgaris* [15, 42]. They also form part of the conductive filament structures

(pili or nanowires) in electro-active microbial cells [43]. Cytochromes (c-type) allow a bacterium to transfer or accept electrons through a redox chain from the metal surface into its cytoplasm [44]. “Cytochrome (c-type)” and “Cytochrome” are used interchangeably in this thesis.

But it should be noted that cytochromes are not the only electron mediators. Other electron mediators include “soluble compounds” that “shuttle” electrons via redox reactions [45]. Bacteria (e.g., *Shewanella oneidensis*) can secrete mediator compounds [20], e.g., Flavin adenine dinucleotide (FAD). These types of soluble compounds secreted by the bacteria are called endogenous mediator compounds [13].

Now, looking back at cytochromes and their ability to transfer electrons, Myers et al. [46] detected high concentrations of cytochromes in the outer membrane (OM) of metal-reducing bacteria (a type of corrosive bacteria) cultured in an anaerobic environment. Also, Myers et al. [46] proposed that the facultative nature of SRBs “enhances the expressions of genes that code for cytochromes” in the OM, which means that a switch to anaerobic conditions from aerobic conditions promotes the development of cytochromes in the OM. And the OM is the part of the bacterium that is attached to the metal.

Myers et al. [46] also reported that since metal-reducing bacteria use Fe(III) or Mn(IV) as terminal electron acceptors, “localized electron transport components in the OM” can facilitate electron transport. Beliaev et al. [23] identified two proteins in the cell membrane of *Shewanella putrefaciens*, which are potentially part of the electron transfer chain for metal-reducing bacteria. Also, Myers et al. [46] proposed that the cytochromes could either

be terminal electron acceptors or intermediaries in an electron transfer link between bacteria and metal. Even though the works of Myers et al. [46, 47] and Beliaev et al. [23] consider gram-negative bacteria, some gram-positive bacteria have also been shown to use direct contact EET mechanism [48]. Gram-negative and positive bacteria are classified under SRB and are thoroughly explained elsewhere [49].

As stated earlier, electroactive bacteria have been used as biocathodes in microbial fuel cells (MFC). One of the MFC biocathode mechanism is based on a microbial cell receiving electrons from the metal (cathode) via its outer cell membrane where cytochromes are present [50]. This MFC biocathode principle is consistent with metals losing electrons to bacteria in MIC.

Venzlaff et al. [19] demonstrated the direct electron consumption by SRB in experimental work, by culturing SRB in an environment where metallic iron was the only electron donor. Venzlaff et al. [19] reported that the cultured SRB consumed electrons from metals via "redox-active cell-associated proteins (cytochromes)" and conductive ferrous sulfide.

Since cytochromes form a redox intermediary for electron transfer between metal and bacteria [51, 52], some SRB can switch to the metal as an energy source when starved off organic carbon source [31, 50]. Taking electrons from metal oxidizes it, thus liberating metal ions (e.g., Fe^{2+}). This oxidation develops anodic sites on the metal surface as pits [53]. Therefore, bacteria consuming electrons from metal sustains the anodic dissolution and influences pit propagation, hence MIC [18].

Nutrients available to SRB will also impact the degree of MIC [14]. Sulfate is a key nutrient for SRB metabolism [3]. SRB metabolism involves using electrons from metals to reduce sulfate when starved off organic carbon energy source [54]. This metabolic reaction is an intracellular process, implied by the BCSR theory. Therefore, electrons from metal and nutrient available to SRB can be limiting factors to MIC propagation.

As part of the corrosion rate predicting process, we propose two cases which include; Case 1, cytochrome being the terminal electron acceptor, thus cytochrome acting as an electron carrier and not an intermediary; and Case 2, Sulfate being the terminal electron acceptor where cytochromes play an intermediary role as has been established. In Case 1, authors of this work acknowledge that cytochromes shuttle electrons periodically between metal and bacteria/biofilm and hence are not technically considered as terminal electron acceptors [15, 46, 55, 56]. However, we attempt to mimic the behavior of protons (H^+), which can also shuttle electrons and in some cases have been considered as terminal electron acceptors in mechanistic models [3, 16]. The aim of this is to compare corrosion rates of sulfate as a terminal electron acceptor with cytochromes assumed as terminal electron acceptors.

3.3 The Mechanistic Model

This model aims at quantifying the corrosion current densities generated from the electron transfer process based on the direct contact EET mechanisms described in MIC. First, we check the thermodynamic feasibility of the redox reactions proposed by the BCSR theory. Then, model the anodic current density considering sulfide conditions in the environment, followed by describing the kinetics of the direct contact EET mechanism to model the

cathodic current densities (i.e., for both cytochromes and sulfate). All variables and data used in the model are defined in Table 3.1.

Metal oxidation and the sulfate reduction according to the BCSR theory is given as [1]:

$$Fe \rightarrow Fe^{2+} + 2e^{-} \quad (3.1)$$

$$SO_4^{2-} + 9H^{+} + 8e^{-} \rightarrow HS^{-} + 4H_2O \quad (3.2)$$

Reaction (3.1) shows the anodic reaction where electrons are released. Reaction (3.2) represents the cathodic reaction that takes place inside the cell cytoplasm [2]. The biofilm is assumed to be the cathode and the metal surface covered by the biofilm is the anode.

The electrochemical cell reaction from the half-cells (3.1) and (3.2) are thermodynamically spontaneous under standard conditions, i.e., pH 7, 25°C, and 1M of solutes [41]. The equilibrium potentials of the half-cell reactions Fe/Fe^{2+} and SO_4^{2+}/ HS^{-} are $-447mV$ and $-217mV$, respectively. This gives a cell potential (E^o_{cell}) of +230mV using equation 3.3. Therefore, the given E^o_{cell} results in -176 kJ mol Gibbs free energy (ΔG^o) under standard conditions [3], this is found using equation 3.4.

$$E^o_{cell} = E_S - E_{Fe} \quad (3.3)$$

$$\Delta G^o = -nFE^o_{cell} \quad (3.4)$$

The Nernst equations, i.e., equations 3.5 and 3.6, can be used to calculate the cell potential of each half-cell reaction to obtain new equilibrium potentials [41].

$$E_{Fe} = -0.447 + \frac{RT}{2F}\ln[Fe^{2+}] \quad (3.5)$$

$$E_S = 0.249 - \frac{2.591RT}{F}pH + \frac{RT}{8F}\ln\frac{[SO_4^{2+}]}{[HS^-]} \quad (3.6)$$

Where;

$E_{Fe} = Fe^{2+}/Fe^0\ couple$

$E_S = SO_4^{2+}/HS^-\ couple$

The thermodynamic feasibility of MIC can then be determined at conditions measured in situ using equations 3.3 to 3.6 but does not provide information on corrosion rate.

Reactions 3.1 and 3.2 involve the flow of charges, and the corrosion rate can be measured by obtaining the current density of the overall cell reaction. The current density of the overall cell reaction is known as corrosion current density (i_{corr}) [57]. Considering the complexity in the MIC process, quantifying the current densities require considering the intermediate redox reactions. The corrosion rate depends on charge transfer and mass transfer of chemical species involved in the redox reaction process.

3.3.1 The anodic current density of Fe/Fe^{2+}

The electrochemical modeling approach by Zheng et al. [58] is adopted to quantify the anodic current density in a sulfide environment. A sulfide environment is assumed because of the evidence of H_2S concentration, and FeS precipitates in many MIC forensics [59]. Fe/Fe^{2+} is assumed to be the only anodic reaction on the metal surface. The Tafel equation for the anodic current density is given as:

$$i_{Fe} = i_{o,Fe} \times 10^{\frac{\eta_{Fe}}{\beta_{Fe}}} \quad (3.7)$$

Where;

$$\beta_{Fe} = \frac{RT \times 2.303}{nF\alpha} \tag{3.8}$$

$$\eta_{Fe} = E_{Fe} - E_{ms} \tag{3.9}$$

Even though it can be argued that the Langmuir adsorption model is used in H_2S corrosion, its premise is to model the effect of sulfide concentration on the anodic exchange current density because HS^- is the preferred adsorbent for Fe^{2+} when concentrations of about 100 ppm of H_2S is traced or detected within the environment [60]. Also, HS^- is a by-product of SRB metabolism and, SRB contributes directly in polluting the environment with H_2S, this makes the Langmuir adsorption model suitable and hence adopted to quantify the anodic exchange current density. The Langmuir adsorption is given as;

$$i_{o,Fe} = i^*_{o,Fe}\theta_{HS^-} e^{\left(-\frac{\Delta H}{R}\left(\frac{1}{T}-\frac{1}{T_{ref}}\right)\right)} \tag{3.10}$$

Where;

$$\theta_{HS^-} = -\frac{K_2 C_{HS^-}}{1+K_2 C_{HS^-}} \tag{3.11}$$

Dissolved H_2S and produced bisulfide (HS^-) reaction is given as;

$$H_2S \leftrightarrow H^+ + HS^- \tag{3.12}$$

By rearranging the equilibrium reaction equation, we can find bisulfide (HS^-) concentration as;

$$[HS^-] = \frac{K_{H_2S}[H_2S]}{[H^+]} \quad (3.13)$$

$$K_{H_2S} = 10^{(782.43945+0.361261\times T - 1.6722\times 10^{-4}\times T^2 - \frac{20565.7315}{T} - 142.74122\times \log(T))} \quad (3.14)$$

3.3.2 Bio-electrochemical Cathodic Reaction

Here we consider the two cases stated earlier, in modeling the cathodic reaction. Case 1 considers the main cathodic reaction to be the cytochrome reduction reaction, where metal loses electrons to the biofilm by cytochromes acting as electron carriers. Case 2 considers sulfate reduction as the main cathodic reaction, however with an exchange current density that depends on the redox intermediary role of cytochrome. We want to reiterate that considering cytochromes as an electron acceptor is an assumption and that it has been well established as an electron transfer intermediary [15, 46, 55, 56]. This assumption is for corrosion rate comparative purposes between sulfate as an electron acceptor and cytochromes as an electron acceptor.

The corrosion in case 1 is expected to be dominated by a charge transfer control process because we have a fixed reducing agent, which is the cytochrome. In Case 2, corrosion is expected to be both charge and mass transfer controlled because the reducing agent is sulfate, which is a soluble chemical species that diffuses through the biofilm to the cathodic site.

Case 1:

The microbes are assumed to be in direct contact with the metal surface. Additionally, we assume that the sessile SRB is starved off organic carbon energy source, thus taking

electrons from the metal. The cytochromes are embedded in the outer membrane cell wall of the bacterium and form a fraction of the sessile bacterium biomass, thus providing an "active layer" for electron transfer [11, 12]. We also assume that the main cathodic reaction causing electron loss from the metal is the cytochrome reduction reaction. The cytochrome is considered a fixed mediator under the direct contact mechanism.

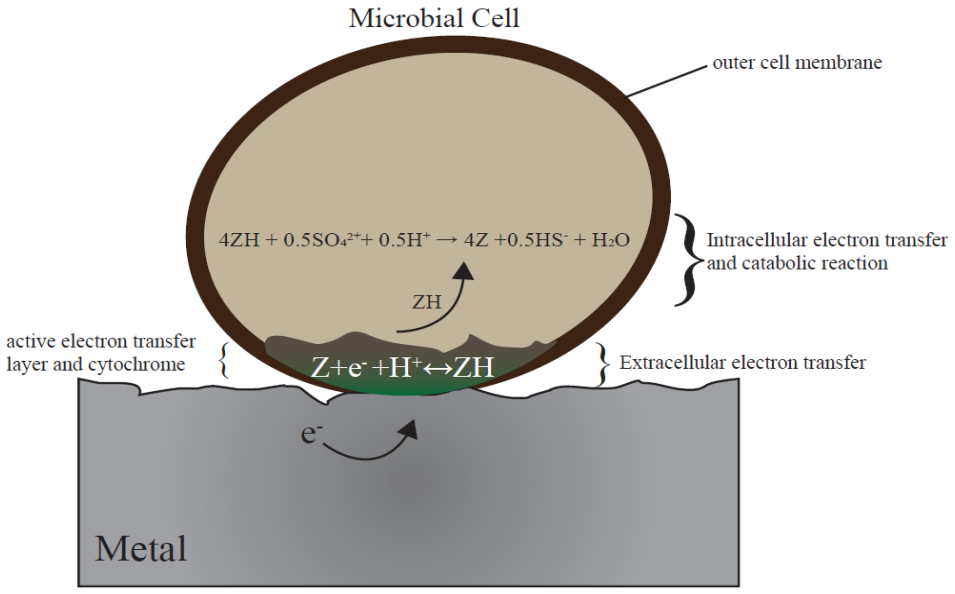

Figure 3.2 An electroactive microbiological cell showing the electron transfer process leading up to sulfate reduction .

From Figure 3.2, the intracellular electron transfer from cytochrome to the electron acceptor (SO_4^{2+}) is facilitated by an enzyme [61]. However, the focus here is that electrons are being held up by cytochromes. Figure 3.3 describes the potential drop (i.e., from a more negative to a less negative potential) across the metal to the biofilm that is driving the electron transfer process described in Figure 3.2. [15].

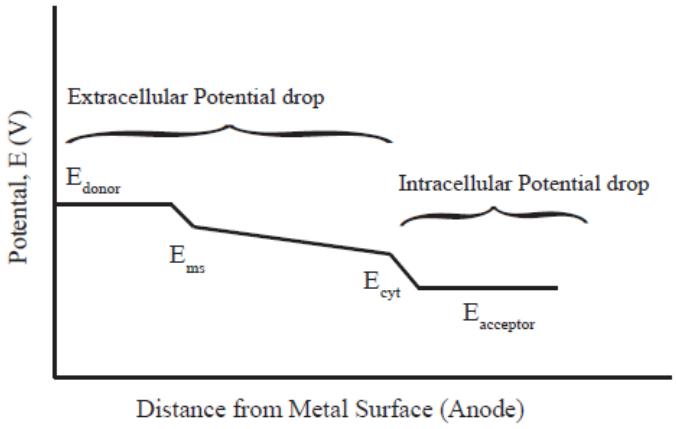

Figure 3.3 The key potential drops driving electron transfer from metal to biofilm. The Extracellular potentials include: $E_{donor} - E_{ms}$ and $E_{ms} - E_{cyt}$, whereas the Intracellular potential drop: $E_{cyt} - E_{acceptor}$, this is catalyzed by an enzyme. Hence, the overall potential drop for the electron transfer is $E_{donor} - E_{acceptor}$. Note: E_{donor}, $E_{acceptor}$, E_{ms} and E_{cyt} are the potentials of electron donor (metal), electron acceptor (sulfate), metal surface and cytochrome, respectively [15].

From Figure 3.3, the overall extracellular potential drop is between E_{donor} and E_{cyt} for case 1. Therefore, the redox property of the microbiological cell outer membrane proteins, i.e., cytochrome, is used to model the cathodic reaction. The Butler-Volmer principle is used to describe the kinetics of EET between the metal surface and the cytochrome. The reaction below shows where the metal finally loses electrons to the cytochrome.

$$Z + e^- + H^+ \leftrightarrow ZH \qquad r_Z \qquad (3.15)$$

r_Z represents the rate of the reversible cytochrome redox reaction.

$$r_Z = k_{f,Z}C_Z - k_{b,Z}C_{ZH} \tag{3.16}$$

$k_{f,Z}$ and $k_{b,Z}$ represents both forward and backward reactions. So, the rate of reaction as a function of potential is given as:

$$k_{f,Z} = k_z^0 exp\left(-\propto \frac{F}{RT}(E_{ms} - E_z)\right) \tag{3.17}$$

$$k_{b,Z} = k_z^0 exp\left((1-\propto)\frac{F}{RT}(E_{ms} - E_z)\right) \tag{3.18}$$

k_z^0 is the rate of electron transfer between cytochrome and biofilm [11]. The rate of electron transfer varies widely due to biodiversity, with rates ranging between 0.001 s^{-1} and 10 s^{-1} [11]. Some experimental work has shown electron transfer rates between metal and bacteria with outer membrane cytochrome to be between 0.03 s^{-1} and 1.2 s^{-1} [62]. E_z is the standard redox potential of cytochromes [61].

By substituting equation 3.17 and 3.18 into 3.16, the rate of electron transfer from metal to biofilm across a potential drop is given as;

$$r_c = k_z^0 L_B\left[C_Z\, exp\left(-\propto \frac{F}{RT}(E_{ms} - E_z)\right) - C_{ZH} exp\left((1-\propto)\frac{F}{RT}(E_{ms} - E_z)\right)\right] \tag{3.19}$$

$Note$: $C_Z \cong C_{ZH}$ because the cytochrome biomass concentration is fixed in its reduced or oxidized form.

Hence, the rate of electron transfer from metal to biofilm is a function of current density across the active charge transfer layer of the biofilm and metal surface potential;

$$r_c = \frac{i_C}{F} \tag{3.20}$$

Therefore, the cathodic current density is given as;

$$i_c = r_c F \tag{3.21}$$

Hence, the exchange current density can be deduced from equation 3.21 as:

$$i_c^0 = k_z^0 L_B C_Z F \tag{3.22}$$

which is a function of cytochrome biomass concentration C_Z, rate of electron transfer k_z^0 and length of active transfer layer L_B [2,11].

Case 2:

The microbiological cells are assumed to be in direct contact with the metal surface, and the sessile SRB is starved off organic carbon energy source, thus taking electrons from metals via cytochromes. Also, we assume that the intracellular electron transfer kinetics is a fast process and happens close to the cell wall. Because the cell wall is attached to the metal surface, we assume that sulfate reduction potential (E_S) drives the cathodic reaction. The exchange current density measures the current generated due to electron transfer between the sessile bacteria and the metal. It depends on many parameters, some of which include the biomass concentration of sessile bacteria directly attached to the metal surface as well as some other enzyme activities [3]. Because sulfate reduction is intracellular, it is reduced by electrons when they are transferred across the cell wall. Therefore, we maintain the exchange current density used in Case 1 which depends on the rate of electron transfer across the cell wall k_z^0, length of the active transfer layer L_B and cytochrome concentration

C_Z. The idea of exchange current density depending on biofilm conductive properties is supported elsewhere [1,2,13].

Now, we replace E_z with E_S in equation 3.19 to account for sulfate reaction potential. And substitute equation 3.19 into equation 3.21. By considering the cathodic side of the equation, the charge transfer controlled cathodic current density is given as:

$$i_{c,SO_4^{2+}} = i_c^0 \, exp\left(-\propto \frac{F}{RT}(E_{ms} - E_S)\right) \tag{3.23}$$

3.3.3 Mass transfer of chemical species

The diffusion equation governs the mass transfer of the chemical species involved in the various electrochemical reactions at the electrodes. In this model the 1-D diffusion equation is adopted. This mass transfer equation is used to obtain the concentration of the chemical species such as H_2S and SO_4^{2+} beneath the biofilm. The diffusion equation is given as [3]:

$$\frac{\partial C_i}{\partial t} = D_i \frac{\partial^2 C_i}{\partial x^2} + R_i \tag{3.24}$$

Where;

$C_i = \text{Concentration of a chemical species, I } (\text{mol/m}^3)$

$D_i = \text{diffusivity constant of a chemical species, I } (\text{m}^2/\text{s})$

$R_i = \text{rate of reaction of diffusing species, i}$

For case 2, we find the limiting current density due to the mass transfer of sulfate to the cathodic site by using equation 3.25:

$$i_{lim} = -nFD_s \frac{dC_s}{dx} \quad (3.25)$$

Where;

$C_s =$ Concentration of a sulfate (mol/m^3)

$D_s =$ diffusivity constant of a sulfate (m^2/s)

Hence the total cathode current density, which accounts for both charge and mass transfer resistance in Case 2 is given as:

$$i_{c_{total}} = \frac{i_c}{1-\frac{i_c}{i_{lim}}} \quad (3.26)$$

The corrosion rate formula for iron (Fe) is given as [2,3]:

Corrosion rate, $^{dP}/_{dt} = 1.155 i_{Fe}$ (3.27)

Table 3.1 Data for the mechanistic model

Parameter Description	**Symbol**	**Value**	**Unit**	**Source**
Fe/Fe^{2+} potential	E_{Fe}	-488	mV	[60]
Enthalpy	ΔH	37.5	kJ/mol	[60]
Anodic reference exchange current density	$i^*_{o,Fe}$	0.33	A/m^2	[60]
Bulk H_2S concentration	C_{H_2S}	20	mmol	chosen
Bulk SO_4^{2+} concentration	C_S	20	mmol	chosen
Reference temperature	T_{ref}	295	K	[60]
Langmuir adsorption model constant	K_2	3.5×10^6	dimensionless	[60]

Sulfate reduction reaction potential	E_S	-217	mV	[3]
Cytochrome concentration	C_Z	3.6×10^{-3}	mol/l	assumed
Cytochrome reduction reaction potential	E_z	-254	mV	[61]
rate of electron transfer (biofilm/electrode)	k_z^0	0.08	s^{-1}	Assumed
length of the active transfer layer	L_B	10^{-3}	m	[11]
SO_4^{2+} diffusivity constant	D_S	0.8×10^{-9}	m^2/s	[63]
H_2S diffusivity constant	D_{H_2S}	1.61×10^{-9}	m^2/s	[63]
Rate of reactions of diffusive species	R_i	0		assumed
Faraday constant	F	96485.34	C/mol	
Coefficient of symmetry	α	0.5	dimensionless	
Universal gas constant	R	8.31	J/mol K	
Temperature	T	298	K	

3.4 Results and Discussion

A biofilm thickness of 20 microns and 20 mmol of both SO_4^{2+} and dissolved H_2S were assumed in the bulk fluid. All reactions were considered at pH = 4, which falls within the optimal range for SRB activity. The equations used to develop the model were solved numerically using MATLAB. Concentrations of SO_4^{2+} and H_2S at the metal surface, beneath the biofilm, were obtained using the mass transport equation, i.e., equation 3.24. Simulated H_2S and SO_4^{2+} concentrations at the metal served as inputs to equations 3.13 and 3.25 respectively.

Potentiodynamic sweeps were simulated at +/-10mV using anodic and cathodic current density equations, i.e., equations 3.10, 3.21 and 3.23. Chemical species concentration served as inputs to the equations used for Potentiodynamic sweep simulations and therefore a time-dependent corrosion potential (E_{corr}) was recorded over 365 days from the anodic and cathodic polarization curve intersections. E_{corr} were used as inputs in equation 3.10 to find corrosion current densities (i_{corr}). Corrosion rates over 365 days were calculated using equation 3.27, with i_{corr} as inputs. Pit depth over 365 days was also calculated from solving the corrosion rate differential equation where pit depth is the dependent variable.

Case 1:

Figure 3.4 shows that corrosion is controlled by charge transfer over a 30-day period, which is the early phase of the corrosion process. Figure 3.5 shows a mass transfer-controlled process, after 300 days. This transition from charge to mass transfer-controlled process correlates well with pit depth increase over time in Figure 3.7. In a sense that, as the pit grows, a void is created between the cell outer membrane and the metal surface. This void/pit short circuits the electron flow from metal to the bacterium, thereby reducing the rate of electron loss from metal. The early phase of corrosion provides an easy flow of electrons from metals (Figure 3.7), and therefore a linear pit propagation is observed until about 150 days where pit growth slows down to a maximum pit depth of about 5.2 mm at day 365.

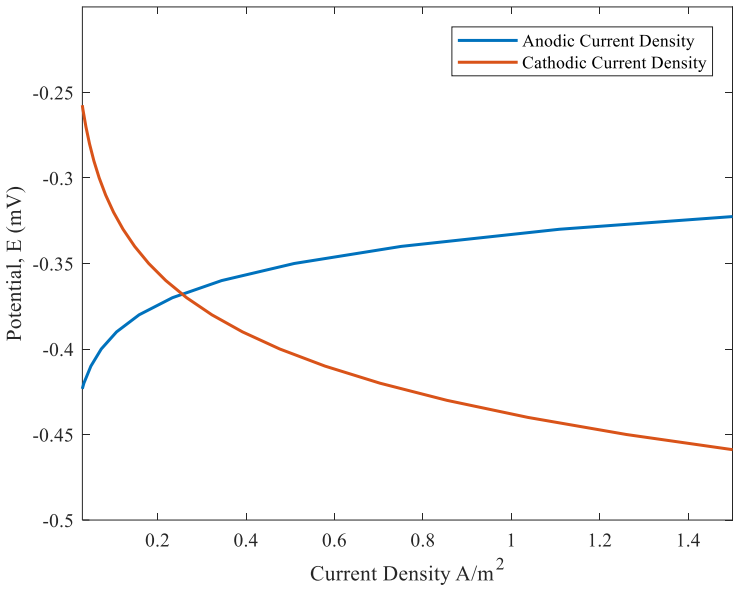

Figure 3.4 Case 1 Potentiodynamic Sweep at 30 days.

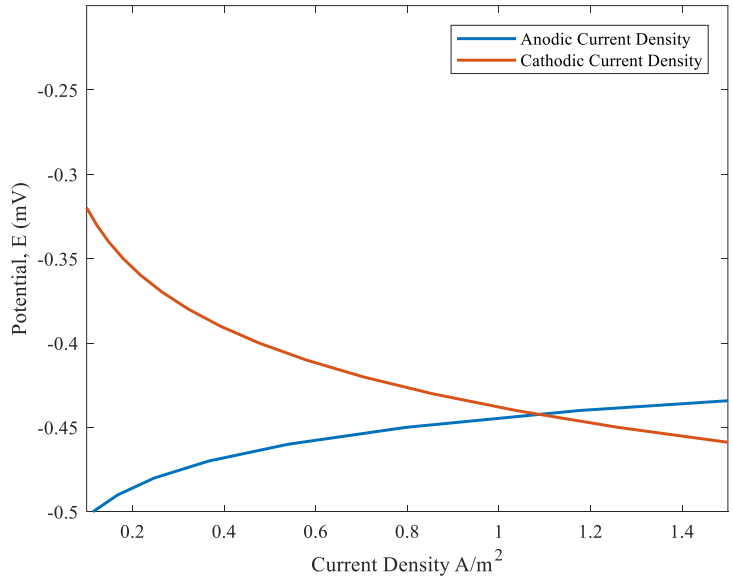

Figure 3.5 Case 1 Potentiodynamic Sweep at day 365.

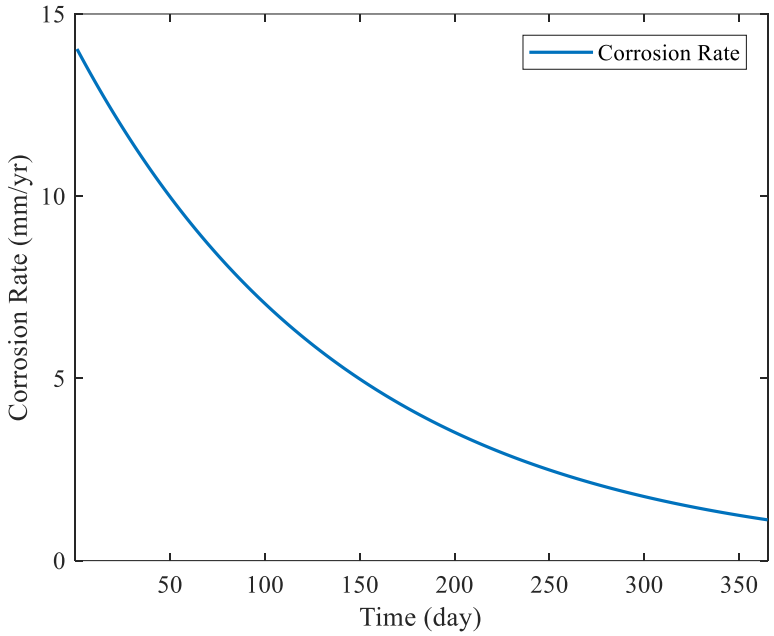

Figure 3.6 Case 1 corrosion rate change over 365 days at anodic sites.

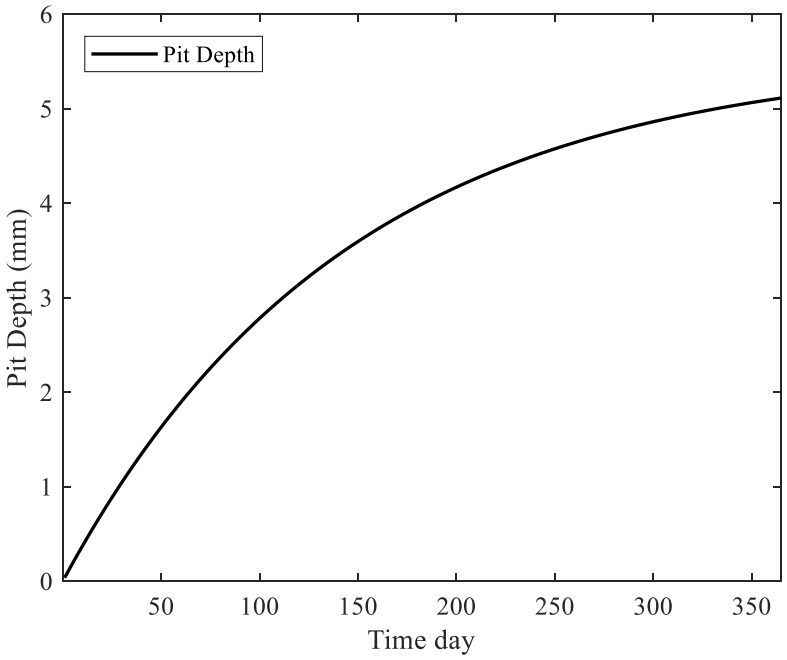

Figure 3.7 Case 1 Pit Depth progression over 365 days.

Case 2:

Figure 3.8 shows corrosion to be controlled by charge transfer in the early phase since the corrosion potential at day 80 is within the charged control region of the anodic curve. The effect of the mass transfer-controlled process is shown in Figure 3.9. The corrosion rate is controlled by mass transfer because the sulfate needed for the cathodic reaction must diffuse through the biofilm to the sessile bacteria in contact with the metal. Hence the cathodic region becomes more negative since excess electrons are accumulated waiting to be used by the bacteria upon the availability of sulfate, which leads to a more negative potential at the cathodic region. A more negative potential is typical to cathodic reactions, whereas a more positive potential is to anodic reactions because metal ions (Fe^{2+}) accumulate within the anodic region.

Figure 3.10 shows a steady decline in the corrosion rate over 365 days. Corrosion decline affects pit growth, as shown in Figure 3.11. A maximum pit depth of about 0.56mm is attained at a plateau after 365 days.

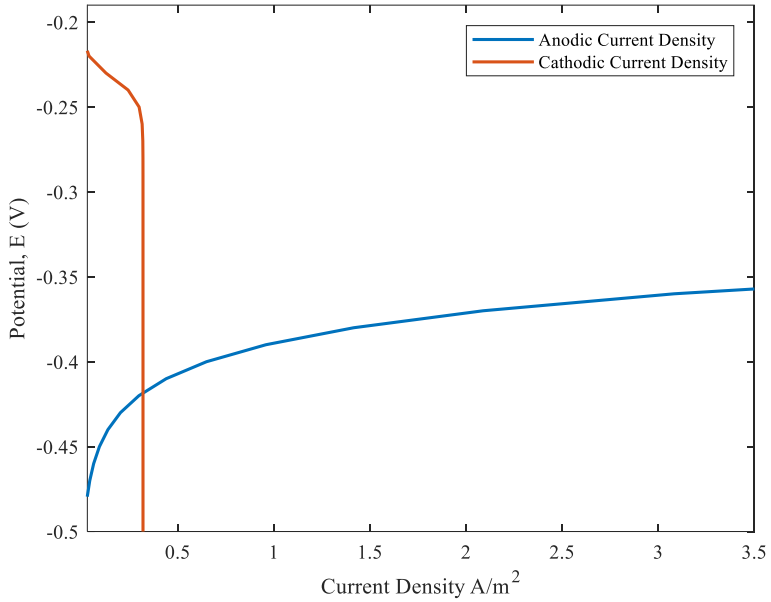

Figure 3.8 Case 2 Simulated potentiodynamic sweep at the early phase (day 80).

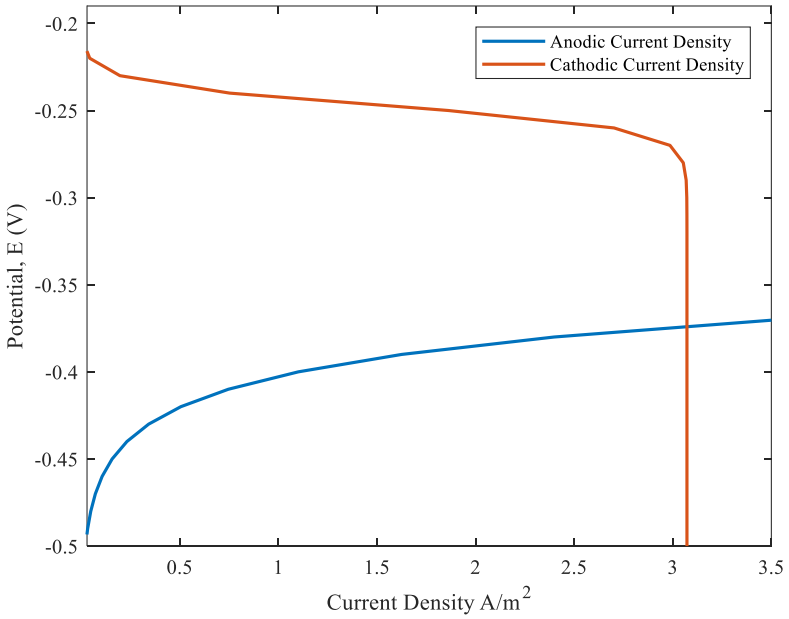

Figure 3.9 Case 2 Potentiodynamic Sweep at day 365.

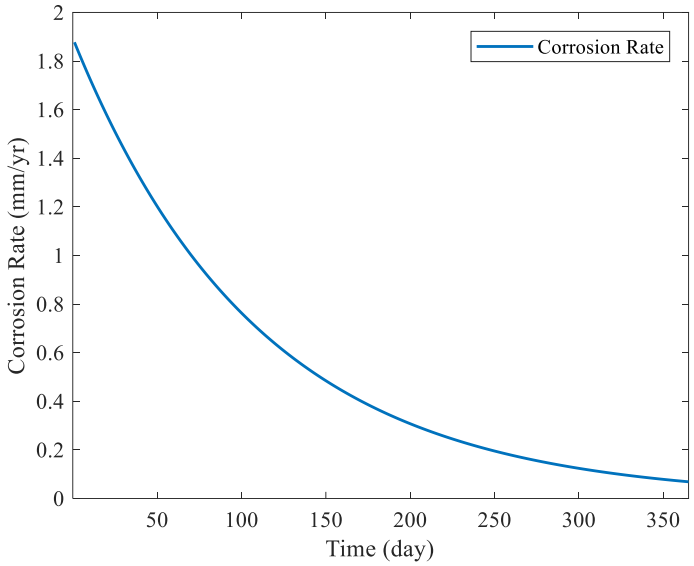

Figure 3.10 Case 2 Corrosion Rate decline due to mass and charge transfer limitation in Sulfate reduction.

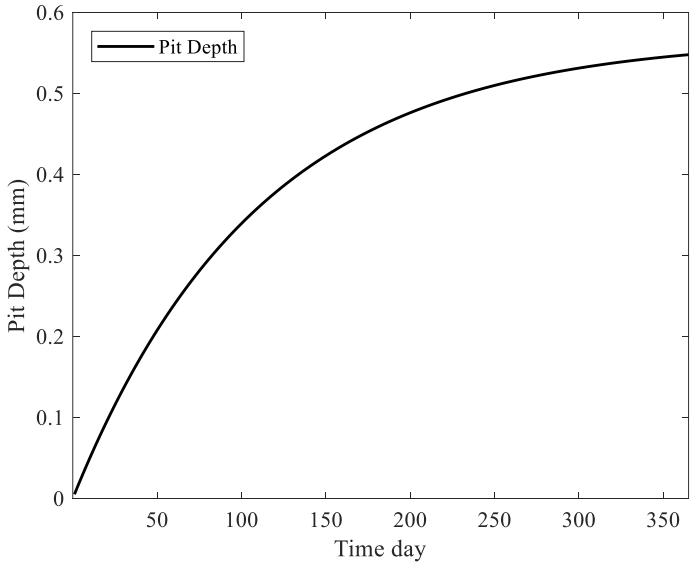

Figure 3.11 Case 2 Pit depth increase with time over 365 days.

3.4.1 Comparing sulfate reduction and cytochrome reduction corrosion rates

In Figure 3.12, we compare the corrosion rate and pit depth trends between Case 1 and Case 2, as proposed earlier, when we assumed cytochrome to be an acceptor. There is evidence of higher corrosion rates in cytochromes reduction as compared to sulfate reduction. However, we observe an extremely high corrosion rate of 5.2 mm/yr for the cytochrome reduction, which is not typical in pure MIC conditions, given how slow the metabolic process is. Nonetheless, the presence of mediators, such as cytochromes in MIC experiments, has shown relatively higher corrosion rates as compared to when they are absent [19,38]. This result affirms the significance of the redox properties of chemical mediators and cytochromes, in that if cytochromes act as “carriers,” and thus temporarily accept electrons without immediately passing them on, they could be significant to MIC propagation.

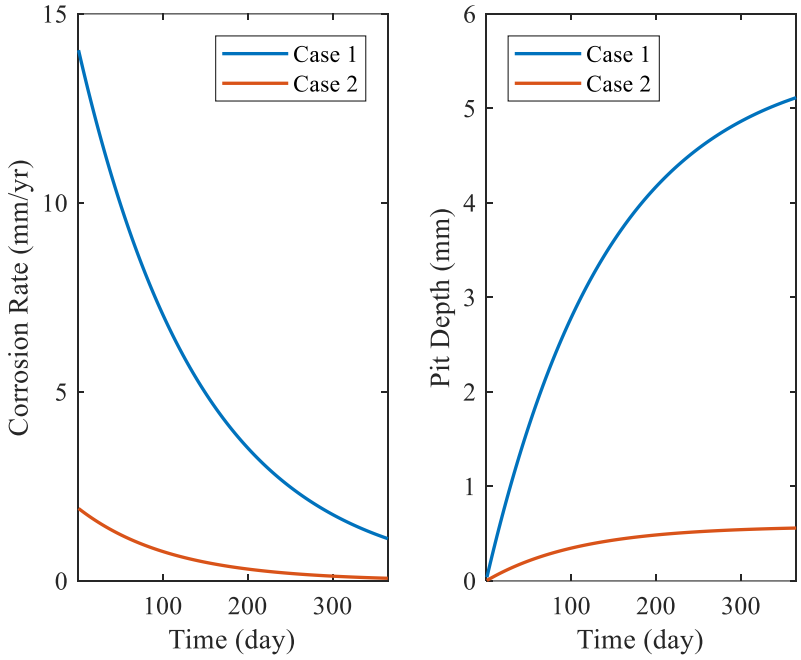

Figure 3.12 Comparing corrosion rate and pit depth propagation between case 1 and 2.

Another reason for corrosion rates in cytochrome reduction being higher than sulfate reduction could be the immediate exposure of the reducing species to the metal surface. In the direct contact EET mechanism, cytochromes are highly exposed to the metal surface, which makes its reduction reaction readily accessible. However, sulfate as a reducing species may not be readily exposed to the metal surface due to biofilm thickness and possible consumption of sulfate by planktonic bacteria in the bulk fluid.

3.4.2 Effect of biofilm thickness on corrosion rate

We further investigate the effect of biofilm thickness on corrosion, by a simulating corrosion rate and pit depth growth and varying biofilm thickness. Figure 3.13 shows the corrosion rates and pit depth growth for a biofilm thickness of 5 microns and 20 microns.

Here we consider case 2 only, where sulfate is the terminal electron acceptor. Also, case 2 represents the well-established electron consumption MIC mechanism for SRB.

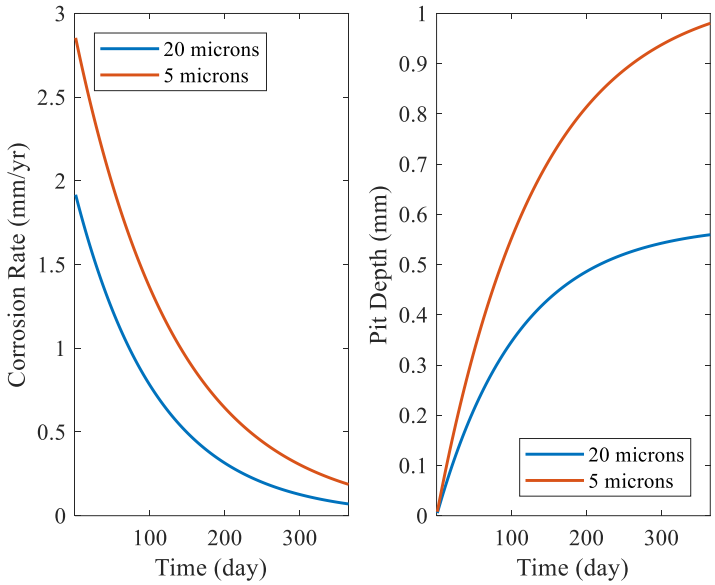

Figure 3.13 Comparing corrosion rate and pit depth propagation between biofilm thicknesses of 5 and 20 microns.

There is significant evidence from these results of a reducing species exposure to the metal surface being a critical factor in MIC propagation. The results show a one-year maximum pit depth of 0.98 mm and 0.56 mm for a biofilm thickness of 5 microns and 20 microns respectively. These pit depths of 0.98mm and 0.56 mm per year, corroborate well with mechanistic studies where iron was the sole electron donor to SRB, in an anaerobic environment. Pit depth per year rate of 0.7 mm/yr. was recorded in this study with no evidence of catalytic enhancement of cathodic hydrogen [19]. Also, the trend in changing corrosion rates over the one-year period shows initial rates being 2.85 mm/yr. for 5 microns

biofilm thickness and 1.92 mm/yr. for 20 microns biofilm thickness within the first 100 days. Corrosion rates declines to 0.18mm/yr. and 0.07mm/yr. for 5 microns and 20 microns biofilm thickness respectively after 365 days.

A low biofilm thickness means that the SRB sessile bacteria close/attached to the metal surface have high exposure to sulfate for its metabolic process as opposed to a thicker biofilm. Biofilm thickness' effect on MIC has been argued extensively in literature [7, 14, 18]; nonetheless, this result provides a quantitative insight to that effect. It also provides insight as to why it is important to pay attention to redox intermediaries directly interfacing the metal whose activities may not directly relate to biofilm metabolism, assuming they are electron carriers. There are several other mechanisms in MIC, including EET mechanisms and chemical MIC mechanisms that can contribute to corrosion in sync with this mechanism highlighted in this work. It should also be noted that the effect of biofilm thickness considered here is only valid with respect to our assumptions, which include, a condition where the bacteria are taking electrons from the metals. Therefore, biofilm thickness may have other effects in other forms of MIC. Nevertheless, we seek to develop a quantitative understanding of these mechanisms systematically by using new knowledge emerging from recent studies in electroactive biofilms, which is still an active research area in tandem with MIC.

3.5 Conclusion

A mechanistic model has been developed to predict MIC rates using the direct contact EET mechanism. Furthermore, a comparative study was done between cytochrome reduction reaction and sulfate reduction reaction. This comparative study aims to measure the impact

of both reducing species on MIC rate. The cytochrome reduction reaction recorded higher corrosion rates as compared to the sulfate reduction reaction by a difference of 4.64 mm/yr.

The effect of reducing species exposure to the electron donor (metal surface) was also investigated. The aim was to understand the higher corrosion rates in cytochrome reduction reactions since they are more exposed to the metal surface. Also, biofilm thickness of 5 microns and 20 microns were simulated for sulfate reduction only. Higher corrosion rates were measured in the 5 microns biofilm as compared to the 20 microns biofilm thickness. These results provide quantitative insight into the effect of reducing species exposure to the metal surface and the thickness of biofilm on MIC. Corrosion rates recorded from the sulfate reduction for based on the effect of biofilm thickness also corroborate well with corrosion rates from experimental work under similar anaerobic conditions where hydrogen as an electron "shuttle" is absent.

Authors of this work will like to clarify that the reliability of the predictions is subject to the assumptions and method considered in this work. This work encourages the exploration and investigation of other electron transport mechanisms in EET to improve on the understanding of MIC and electron loss in metals. Though the modeling approach used in this work is applied extensively in modeling bioanodes in MFCs, the electron transfer process in EET is reversible given the use of biocathodes; hence we adopt this method to model electron transfer from metal into biofilm, where biofilms represent biocathodes.

3.6 References

[1] . T. Gu, K. Zhao, S. Nesic, A new mechanistic model for mic based on a biocatalytic cathodic sulfate reduction theory, NACE - International Corrosion Conference Series (2009).

[2] T. Gu, Theoretical Modeling of the Possibility of Acid Producing Bacteria Causing Fast Pitting Biocorrosion, Journal of Microbial and Biochemical Technology. 6 (2014) 68-74.

[3] D. Xu, Y. Li, T. Gu, Mechanistic modeling of biocorrosion caused by biofilms of sulfate reducing bacteria and acid producing bacteria, Bioelectrochemistry. 110 (2016) 52-58.

[4] S. Al-Jaroudi, A. Ul-Hamid, M. Al-Gahtani, Failure of crude oil pipeline due to microbiologically induced corrosion, Corrosion Engineering, Science, and Technology. 46 (2011) 568-579.

[5] M. Taleb-Berrouane, F. Khan, K. Hawboldt, R. Eckert, T.L. Skovhus, Model for microbiologically influenced corrosion potential assessment for the oil and gas industry, Corrosion Engineering, Science and Technology (2018) 1-15.

[6] T.L. Skovhus, D. Enning, J.S. Lee, Microbiologically Influenced Corrosion in the Upstream Oil and Gas Industry, CRC Press, 2017.

[7] B.J. Little, J.S. Lee, Microbiologically influenced corrosion, John Wiley & Sons, 2007.

[8] . K.B. SÃ¸rensen, U.S. Thomsen, S. Juhler, J. Larsen, Cost efficient MIC management system based on molecular microbiological methods, NACE - International Corrosion Conference Series. 1 (2012) 472-486.

[9] . A.Y. Adesina, I.K. Aliyu, F. Al-Abbas, Microbiologically influenced corrosion (MIC) challenges in unconventional gas fields, NACE - International Corrosion Conference Series. 2015-January (2015).

[10] Y. Li, D. Xu, C. Chen, X. Li, R. Jia, D. Zhang, W. Sand, F. Wang, T. Gu, Anaerobic microbiologically influenced corrosion mechanisms interpreted using bioenergetics and bioelectrochemistry: a review, Journal of materials science & technology (2018).

[11] B. Korth, L.F. Rosa, F. Harnisch, C. Picioreanu, A framework for modeling electroactive microbial biofilms performing direct electron transfer, Bioelectrochemistry. 106 (2015) 194-206.

[12] R. Renslow, J. Babauta, A. Kuprat, J. Schenk, C. Ivory, J. Fredrickson, H. Beyenal, Modeling biofilms with dual extracellular electron transfer mechanisms, Physical Chemistry Chemical Physics. 15 (2013) 19262-19283.

[13] P. Zhang, D. Xu, Y. Li, K. Yang, T. Gu, Electron mediators accelerate the microbiologically influenced corrosion of 304 stainless steel by the Desulfovibrio vulgaris biofilm, Bioelectrochemistry. 101 (2015) 14-21.

[14] T. Gu, D. Xu, Demystifying MIC mechanisms, CORROSION 2010 (2010).

[15] C.I. Torres, A.K. Marcus, H. Lee, P. Parameswaran, R. Krajmalnik-Brown, B.E. Rittmann, A kinetic perspective on extracellular electron transfer by anode-respiring bacteria, FEMS Microbiol. Rev. 34 (2010) 3-17.

[16] . T. Gu, Can acid producing bacteria be responsible for very fast MIC pitting?, NACE - International Corrosion Conference Series. 2 (2012) 1481-1493.

[17] R. Javaherdashti, Microbiologically influenced corrosion: an engineering insight, Springer, 2016.

[18] T. Gu, New understandings of biocorrosion mechanisms and their classifications, Journal of Microbial and Biochemical Technology. 4 (2012) iii-vi.

[19] H. Venzlaff, D. Enning, J. Srinivasan, K.J.J. Mayrhofer, A.W. Hassel, F. Widdel, M. Stratmann, Accelerated cathodic reaction in microbial corrosion of iron due to direct electron uptake by sulfate-reducing bacteria, Corros. Sci. 66 (2013) 88-96.

[20] E. Marsili, D.B. Baron, I.D. Shikhare, D. Coursolle, J.A. Gralnick, D.R. Bond, Shewanella secretes flavins that mediate extracellular electron transfer, Proc. Natl. Acad. Sci. U. S. A. 105 (2008) 3968-3973.

[21] R.S. Renslow, J.T. Babauta, P.D. Majors, H. Beyenal, Diffusion in biofilms respiring on electrodes, Energy & environmental science. 6 (2013) 595-607.

[22] D.K. Newman, R. Kolter, A role for excreted quinones in extracellular electron transfer, Nature. 405 (2000) 94.

[23] A.S. Beliaev, D.A. Saffarini, J.L. McLaughlin, D. Hunnicutt, MtrC, an outer membrane decahaem c cytochrome required for metal reduction in Shewanella putrefaciens MR-1, Mol. Microbiol. 39 (2001) 722-730.

[24] . T. Gu, D. Xu, Why are some microbes corrosive and some not?, NACE - International Corrosion Conference Series (2013).

[25] H. Allen, O. Hill, N.I. Hunt, [19] Direct and indirect electrochemical investigations of metalloenzymes, in: Methods in enzymology, Elsevier, 1993, pp. 501-522.

[26] G. Reguera, K.D. McCarthy, T. Mehta, J.S. Nicoll, M.T. Tuominen, D.R. Lovley, Extracellular electron transfer via microbial nanowires, Nature. 435 (2005) 1098.

[27] G. Reguera, K.P. Nevin, J.S. Nicoll, S.F. Covalla, T.L. Woodard, D.R. Lovley, Biofilm, and nanowire production leads to increased current in Geobacter sulfurreducens fuel cells, Appl. Environ. Microbiol. 72 (2006) 7345-7348.

[28] K.M. Fischer, D.J. Batstone, M.C. van Loosdrecht, C. Picioreanu, A mathematical model for electrochemically active filamentous sulfide-oxidising bacteria, Bioelectrochemistry. 102 (2015) 10-20.

[29] M.Y. El-Naggar, Y.A. Gorby, W. Xia, K.H. Nealson, The molecular density of states in bacterial nanowires, Biophys. J. 95, (2008) L10-L12.

[30] H. Richter, K.P. Nevin, H. Jia, D.A. Lowy, D.R. Lovley, L.M. Tender, Cyclic voltammetry of biofilms of wild type and mutant Geobacter sulfurreducens on fuel cell anodes indicates possible roles of OmcB, OmcZ, type IV pili, and protons in extracellular electron transfer, Energy & Environmental Science. 2 (2009) 506-516.

[31] H. Li, D. Xu, Y. Li, H. Feng, Z. Liu, X. Li, T. Gu, K. Yang, Extracellular electron transfer is a bottleneck in the microbiologically influenced corrosion of C1018 Carbon steel by the biofilm of sulfate-reducing bacterium Desulfovibrio vulgaris, PLoS ONE. 10 (2015).

[32] Y. Li, D. Xu, C. Chen, X. Li, R. Jia, D. Zhang, W. Sand, F. Wang, T. Gu, Anaerobic microbiologically influenced corrosion mechanisms interpreted using bioenergetics and bioelectrochemistry: A review, Journal of Materials Science and Technology (2018).

[33] I.B. Beech, J. Sunner, Biocorrosion: Towards understanding interactions between biofilms and metals, Curr. Opin. Biotechnol. 15 (2004) 181-186.

[34] P. Halkjaer Nielsen, Biofilm dynamics and kinetics during high-rate sulfate reduction under anaerobic conditions, Appl. Environ. Microbiol. 53 (1987) 27-32.

[35] H. Flemming, P.S. Murthy, R. Venkatesan, K. Cooksey, Marine and industrial biofouling, Springer, 2009.

[36] K.M. Usher, A.H. Kaksonen, I. Cole, D. Marney, Critical review: Microbially influenced corrosion of buried carbon steel pipes, International Biodeterioration, and Biodegradation. 93 (2014) 84-106.

[37] C.M. Plugge, W. Zhang, J.C.M. Scholten, A.J.M. Stams, Metabolic flexibility of sulfate-reducing bacteria, Frontiers in Microbiology. 2 (2011).

[38] P. Zhang, D. Xu, Y. Li, K. Yang, T. Gu, Electron mediators accelerate the microbiologically influenced corrosion of 304 stainless steel by the Desulfovibrio vulgaris biofilm, Bioelectrochemistry. 101 (2015) 14-21.

[39] W. Hamilton, Microbially influenced corrosion as a model system for the study of metal microbe interactions: a unifying electron transfer hypothesis, Biofouling. 19 (2003) 65-76.

[40] J.M. Odom, H.D. Peck Jr, Hydrogenase, electron-transfer proteins, and energy coupling in the sulfate-reducing bacteria Desulfovibrio, Annu. Rev. Microbiol. 38 (1984) 551-592.

[41] D. Xu, Y. Li, F. Song, T. Gu, Laboratory investigation of microbiologically influenced corrosion of C1018 carbon steel by nitrate reducing bacterium Bacillus licheniformis, Corros. Sci. 77 (2013) 385-390.

[42] L. Shi, H. Dong, G. Reguera, H. Beyenal, A. Lu, J. Liu, H. Yu, J.K. Fredrickson, Extracellular electron transfer mechanisms between microorganisms and minerals, Nature Reviews Microbiology. 14, (2016) 651.

[43] B.E. Rittmann, Opportunities for renewable bioenergy using microorganisms, Biotechnol. Bioeng. 100 (2008) 203-212.

[44] R.A. Rozendal, A.W. Jeremiasse, H.V. Hamelers, C.J. Buisman, Hydrogen production with a microbial biocathode, Environ. Sci. Technol. 42 (2007) 629-634.

[45] H. Durliat, M. Barrau, M. Comtat, FAD used as a mediator in the electron transfer between platinum and several biomolecules, Journal of Electroanalytical Chemistry and Interfacial Electrochemistry. 253 (1988) 413-423.

[46] C.R. Myers, J.M. Myers, Localization of cytochromes to the outer membrane of anaerobically grown Shewanella putrefaciens MR-1, J. Bacteriol. 174 (1992) 3429-3438.

[47] C.R. Myers, J.M. Myers, Ferric reductase is associated with the membranes of anaerobically grown Shewanella putrefaciens MR-1, FEMS Microbiol. Lett. 108 (1993) 15-22.

[48] A. Cournet, M. Délia, A. Bergel, C. Roques, M. Bergé, Electrochemical reduction of oxygen catalyzed by a wide range of bacteria including Gram-positive, Electrochemistry Communications. 12 (2010) 505-508.

[49] H.F. Castro, N.H. Williams, A. Ogram, Phylogeny of sulfate-reducing bacteria, FEMS Microbiol. Ecol. 31 (2000) 1-9.

[50] L. Huang, J.M. Regan, X. Quan, Electron transfer mechanisms, new applications, and performance of biocathode microbial fuel cells, Bioresour. Technol. 102 (2011) 316-323.

[51] Y.A. Gorby, S. Yanina, J.S. McLean, K.M. Rosso, D. Moyles, A. Dohnalkova, T.J. Beveridge, I.S. Chang, B.H. Kim, K.S. Kim, D.E. Culley, S.B. Reed, M.F. Romine, D.A. Saffarini, E.A. Hill, L. Shi, D.A. Elias, D.W. Kennedy, G. Pinchuk, K. Watanabe, S. Ishii, B. Logan, K.H. Nealson, J.K. Fredrickson, Electrically conductive bacterial nanowires produced by Shewanella oneidensis strain MR-1 and other microorganisms, Proc. Natl. Acad. Sci. U. S. A. 103 (2006) 11358-11363.

[52] R. Jia, D. Yang, D. Xu, T. Gu, Electron transfer mediators accelerated the microbiologically influence corrosion against carbon steel by nitrate reducing Pseudomonas aeruginosa biofilm, Bioelectrochemistry. 118 (2017) 38-46.

[53] A.J. Bard, L.R. Faulkner, J. Leddy, C.G. Zoski, Electrochemical methods: fundamentals and applications, wiley New York, 1980.

[54] P. Zhang, D. Xu, Y. Li, K. Yang, T. Gu, Electron mediators accelerate the microbiologically influenced corrosion of 304 stainless steel by the Desulfovibrio vulgaris biofilm, Bioelectrochemistry. 101 (2015) 14-21.

[55] D.R. Lovley, The microbe electric: conversion of organic matter to electricity, Curr. Opin. Biotechnol. 19 (2008) 564-571.

[56] A. Okamoto, K. Hashimoto, R. Nakamura, Long-range electron conduction of Shewanella biofilms mediated by outer membrane C-type cytochromes, Bioelectrochemistry. 85 (2012) 61-65.

[57] V.S. Bagotsky, Fundamentals of electrochemistry, John Wiley & Sons, 2005.

[58] Y. Zheng, J. Ning, B. Brown, S. Nešić, Electrochemical model of mild steel corrosion in a mixed H2S/CO2 aqueous environment in the absence of protective corrosion product layers, Corrosion. 71 (2014) 316-325.

[59] A. Ibrahim, K. Hawboldt, C. Bottaro, F. Khan, Review and analysis of microbiologically influenced corrosion: the chemical environment in oil and gas facilities, Corrosion Engineering, Science, and Technology. 53 (2018) 549-563.

[60] Y. Zheng, B. Brown, S. Nešić, Electrochemical study and modeling of H2S corrosion of mild steel, Corrosion. 70 (2013) 351-365.

[61] K. Fischer, Mathematical modelling of electron transfer modes in electroactive microorganisms (2017).

[62] H.K. Ly, F. Harnisch, S. Hong, U. Schröder, P. Hildebrandt, D. Millo, Unraveling the Interfacial Electron Transfer Dynamics of Electroactive Microbial Biofilms Using Surface-Enhanced Raman Spectroscopy, ChemSusChem. 6 (2013) 487-492.

[63] S. Nesic, M. Nordsveen, A. Stangel, A Mechanistic Model for C02 Corrosion with Protective Iron Carbonate Films (2001).

Chapter 4

A probabilistic model for predicting and analyzing Microbiologically Influenced Corrosion (MIC)

Preface

This manuscript has been submitted to CORROSION Journal and is currently under review. I am the first author of this manuscript, and Dr. Faisal Khan is the corresponding author. Mohammed Taleb-berrouane is the second author of this manuscript. I developed the probabilistic model, implemented the model using data from literature, and tested the model's results against existing results from a MIC case study. Dr. Faisal Khan reviewed the model, its results, and provided constructive feedback which was crucial to the improvement of the model. Mohammed Taleb-berrouane reviewed and suggested improvements on the Bayesian theories and manuscript organization. The feedback and suggestions from the co-authors were vital in the development of the final draft of the manuscript.

Abstract

Predicting and analyzing corrosion rate is a challenging process in cases where microbiological influence is suspected. Current predictive models have focused on predicting corrosion rates and pit depth propagation without considering a thorough analysis of the parameters or conditions influencing or limiting the expected corrosion rate. This challenge is partly due to the use of a rigid mechanistic approach in developing predictive models. This work proposes a methodology for predicting corrosion and

analyzing the factors critical to the corrosion rate by using a probabilistic approach. The proposed model uses a fully parameterized Bayesian network made up of 45 nodes. The model is tested by using a MIC case study, which predicts a corrosion rate of 0.3-0.6mm/yr. The analysis shows Iron-Oxidizing Bacteria and Methanogens metabolism contributing mainly to the predicted corrosion rate. The study also provides a list of parameters (factors) to which the predicted corrosion rate is most sensitive to. The application of this model will improve our understanding of the factors impacting MIC and allow operators to predict the corrosion rate in a process system better.

4.1 Introduction

Predicting Microbiologically Influenced Corrosion (MIC) remains a challenge due to the complex microbiological and electrochemical reactions involved in the process [1, 2]. MIC is mostly associated with bacteria metabolism since metabolic products can initiate or promote electrochemical reactions within an environment [3, 4].

These microbiological and electrochemical reactions are a concern because they can cause corrosion in process facilities. For instance, sulfur-producing bacteria can cause H_2S corrosion in pipelines and wellbores [5]. A 25.5 km pipeline transporting light crude, failed after three years of service due to MIC influenced by the metabolism of Sulphate Reducing Bacteria (SRB) [6]. About 77% of oil-producing wells in the United States are affected by MIC [7]. For operators to mitigate some of these concerns, it is vital to track and predict MIC rates.

Predicting MIC rates is important to mitigate the risks involved. In recent years, mechanistic models have been developed to investigate microbiological corrosion rate progression. Mechanistic models are often a preferred method of predicting MIC rate because it can give reliable predictions [8]. However, this makes mechanistic models more rigid and requires a lot of assumptions to reduce complexity.

Gu et al. [9] developed a mechanistic model to predict pit progression due to MIC. The model is based on the Biocatalytic Sulfate Reduction (BCSR) theory. The model assumes only a Sulfate Reducing Bacteria (SRB) biofilm. It focuses on SRB metabolism driving the cathodic reaction process and can predict corrosion rate and pit depth propagation. Gu [10] further developed a mechanistic model to investigate Acid Producing Bacteria (APB). The model investigates how rapid APBs cause corrosion. Xu et al. [11] improved on the works of Gu et al. [9, 10] by developing a mechanistic model which involved both SRB and APB. This model aims at predicting pit propagation as well. Al-Darbi et al. [12] developed a mechanistic model to predict corrosion rate and pit progression. Their model investigates nutrient as a controlling factor in MIC.

Similarly, Peng et al. [13] earlier developed a mechanistic model where nutrient availability to corrosive microbes control MIC. Marciales et al. [8] reviewed several models that have been used to predict MIC rate. Table 4.1 shows a summary of the mechanistic models based on Marciales et al. [8] review and other mechanistic models developed in literature [9, 11-13].

Even though the models in Table 4.1 have improved on the understanding of the mechanisms involved in MIC, this method requires many assumptions to make the model simple. But this approach introduces many uncertainties into the model. Besides, a predictive model is more suitable if it can analyze a wide range of independent factors that influence the corrosion rate predicted. This approach is not applicable in mechanistic models since it requires fewer parameters (factors) to reduce complexity. These shortcomings leave most mechanistic models analyzing only corrosion rate trends under ideal conditions.

This work proposes a practical methodology to predict MIC and further analyze how parameters (i.e., operating conditions and factors) influence the expected corrosion rate. Thus, a flexible modeling approach is needed. Probabilistic graphical models provide such flexibility to achieve the purpose of this work. The primary graphical models include; Bayesian networks (BN) and Markov chains [14]. A Bayesian network enables us to establish a joint probability distribution of random variables [15]. These random variables represent nodes in a directed acyclic graph, where arcs are used to show the dependencies between random variables [16]. A Markov chain is an undirected graph, which also represents the random variables as nodes in a network. Markov chains do not establish an explicit cause-effect relationship between nodes like Bayesian networks [14]. Both models are widely used as predictive tools, especially in safety and risk analysis [17-21].

Here, a BN is adopted to develop a predictive model. Techniques such as Importance Analysis and Sensitivity analysis are used to identify the parameters that influence the corrosion rate predicted. This model uses information from case studies and various MIC

mechanisms that have been thoroughly studied in literature and experiments. Using a BN will allow us to implement many mechanisms and factors that mechanistic models may not consider.

Table 4.1 A summary of Mechanistic models and their characteristics.

Considered Factors	Microbiological Organism(s)	Model Characteristics			Author/ Reference
		Output(s)	Pros	Cons	
Sulfate diffusivity and mass transfer Butler-Volmer Equation	Sulfate Reducing Bacteria (SRB)	Pitting rate Pit depth progression	The model considers the effect of mass and charges transfer resistance of corrosive species across the biofilm layer.	The model considers only an SRB biofilm. The model does not account for SRB metabolism	Gu, Zhao, Nesic [9]
Sulfate diffusivity and mass transfer Butler-Volmer Equation Tafel Equations for calculating current densities (Anodic and Cathodic)	Sulfate Reducing Bacteria (SRB) Acid Producing Bacteria (APB)	Pitting rate	The model considers the effect of mass and charges transfer resistance of corrosive species across the biofilm layer. The model considers the reduction of acetic acid	The model did not account for SRB and APB metabolic growth.	Gu [10]
Butler-Volmer Equation. Tafel Equations for calculating current densities (Anodic and Cathodic)	Sulfate Reducing Bacteria (SRB) Acid Producing Bacteria (APB)	Corrosion rate	The model considers the influence of APB and SRB. The model considers the effect of mass and charge transfer resistance of	A short term SRB corrosion rate data was used to calibrate long term corrosion rate.	Xu, Li and Gu [11]

			corrosive species across the biofilm layer.		
Sulfate diffusivity over biofilm Monod Kinetics equation Constant biofilm thickness and density	Sulfate Reducing Bacteria (SRB)	Corrosion rate	Mass transfer of key nutrient species is considered. SRB growth kinetics was modeled in an existing pit using Monod equations The model is validated with experimental data	The model considers only SRB for corrosion rate prediction	Al-Darbi, Agha, and Islam [12]
Constant biofilm thickness and density Sulfate diffusivity over biofilm Monod Kinetics equation	Sulfate Reducing Bacteria (SRB)	Corrosion rate	The model is validated with laboratory corrosion test data SRB growth kinetics was modeled in an existing pit using Monod equations Mass transfer of essential nutrient across biofilm to sessile bacteria is considered.	The model considers only SRB for corrosion rate prediction	Peng, Seun, and Park [13]

4.2 Link Between Microbiological Metabolism and Corrosion

In this section, we discuss what corrosion is, the microorganisms commonly associated with MIC and how they can cause corrosion. A link between bacteria activities and corrosion is established, focusing on how the metabolism of these bacteria types cause corrosion. We show the effect of process operating conditions in pipelines on bacteria and corrosion.

4.2.1 General Corrosion Concept

Corrosion is the degradation of materials due to its electrochemical and chemical reaction within its environment [22]. Electrons bond a pure metal at its molecular level under high energy. This tight bond gives the metal its hardness. The removal of these electrons from the bonding the metal surface oxidizes the metal ion and liberates it. The electron loss causes the material to degrade [23]. For corrosion to occur, an anode, cathode, electrolyte, and a conductive path for electron transfer are required [24]. The metal losing its electrons is known as the anodic reaction, whereas an ionized chemical species accepting the electrons is known as the cathodic reactions [25]. During corrosion, charges and chemical compounds are transported under various phenomena through the electrolyte to and from cathodic and anodic reaction sites. So once corrosion is initiated, it is sustained by a cathodic species. Hence the principle is that all possible cathodic reactions drive anodic dissolution of metal due to charge and mass transfer of electrons chemical species respectively from anode to cathode. The flow of charges across the metal surface produces anodic and cathodic current densities. This is mathematically represented as [25, 26]:

$$\sum i_a = \sum i_c \tag{4.1}$$

Where;

$i_a = anodic\ current\ density$

$i_c = cathodic\ current\ density$

The Butler-Volmer principle models the current densities at the anodic and cathodic regions of on the metal surface. The reader is referred to the following sources [25, 27, 28] for a detailed kinetic description of the electrochemical process. Below is a representation of a simple corrosion reaction;

Anodic Reaction:

$M \leftrightarrow M^+ + e^-$ (Metal oxidation) (4.2)

Cathodic Reaction:

$Red^+ + e^- \leftrightarrow Red$ (Reduction reaction) (4.3)

4.2.2 Effects of operating and environmental conditions on alloys/metals in corrosion

The environment influences corrosion by providing the conditions necessary (concentration of reacting species, temperature, pH, etc.) for electrochemical reactions. The concentration of the oxidizing and reducing species and electrons from the metal can control the electrochemical reactions when they are in limited supply. This is described in two ways known as mass transfer and charge transfer controlled reactions. Charge transfer controlled reactions is when the transfer of electrons to the cathode is the limiting step in the electrochemical reaction [29]. In a charged transfer-controlled reaction, the concentration of the chemical species is not a rate-limiting step, because, the rate of

corrosion is controlled by the flow of electrons. When the electrochemical reaction is charged transfer controlled, the corrosion rate is rapid because electron transfer is a fast process [11].

Conversely, the mass transfer-controlled reaction is when the concentration of the reacting species controls the electrochemical reaction [25]. This type of controlled reaction is relatively slower since reacting species must diffuse to the cathodic site for the reduction reaction. In real conditions, both controlled reactions occur [28]. In MIC, nutrients species such as sulfate (SO_4^{2+}) can be the reducing species when considering SRB metabolism. The mass transfer-controlled reaction is mostly induced by the biofilm since it controls the rate at which the reducing species (nutrients required by sessile bacteria) diffuse [30]. The controlling processes in the electrochemical reactions are critical to predicting corrosion rates because they enable us to understand how fast or slow the corrosion rate is.

The type of material (metal/alloy) used in a pipeline processing facility can also affect corrosion rates. Carbon steel is a common alloy used in most pipeline processing facilities. Corrosion-resistive alloys (CRA) have been used in harsh operations where carbon steel may fail due to corrosion [31]. Knowing the pit resistance number (PREN) of an alloy allows practitioners to assess materials during selection. PREN is a simple calculation used to determine the resistance of a material to corrosion [2]. Its parameters include; Chromium, Molybdenum, and Nitrogen.

$$PREN = \%Cr + 3.3 \times \%Mo + 16 \times \%N \quad (4.4)$$

A high PREN of an alloy shows high resistance to pitting corrosion. High PREN in alloys has been reported to have low MIC rates upon exposure [32].

Welded surfaces on metal are highly susceptible to corrosion. Unfortunately, welding is ubiquitous in pipeline maintenance. Welding is usually done for repair or joining two or more pipes or materials together. This process leaves the surface rough and prone to biofilm attachment. A surface roughness higher than 3.3µm is highly susceptible to bacteria attachment [2, 33]. Sometimes it is difficult to apply coatings and paintings on welded surfaces, thereby leaving uncoated portions on the metal surface exposed to corrosion attacks.

4.2.3 Bacteria Metabolism and Corrosion

Some of the bacteria common to MIC are categorized into groups known as; Sulfate Reducing Bacteria (SRB), Acid Producing Bacteria (APB), Methanogens, Iron-Oxidizing Bacteria (IOB) and Iron Producing Bacteria (IRB). Their metabolism requires nutrients and an energy source (electrons) [1]. The metabolism of these bacteria can contribute directly and indirectly to corrosion [11]. A direct effect of bacteria metabolism to corrosion is when bacteria take up an electron from the metal surface as an energy source when there is no organic carbon source to supply the bacteria with electrons (e.g., Lactate providing electrons to SRB) [4]. This lithotrophic behavior is typical of SRB (e.g., *Geobacter sulfurreducens* and *Shewanella oneidensis*). Indirectly, bacteria metabolism can cause corrosion when metabolic by-products become active cathodic reactants [3]. Here, we discuss how the metabolism of these bacteria types cause corrosion.

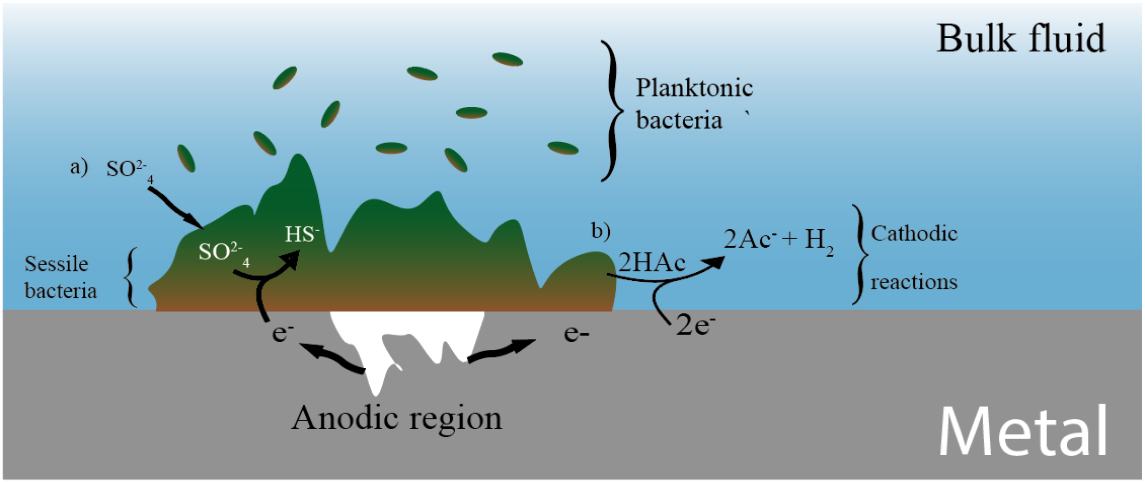

Figure 4.1 A MIC process in an environment showing both direct and indirect electron uptake in (a) and (b) respectively [2]. a) Sulfate diffusing into the biofilm and subsequently reduced by SRB inside the biofilm using electrons from the anode. b) Reduction of acetic acid (APB metabolic end-product) using electrons from the anode.

4.2.2.1 Sulfate Reducing Bacteria (SRB) metabolism and influence on corrosion

The BCSR theory provides a simple explanation of how SRB cause corrosion. The critical nutrient for SRB metabolism is sulfate. SRB electrochemically reduces sulfate in its metabolic process [26]. So, the BCSR theory proposes that SRB can consume electrons from the metal surface to facilitate sulfate reduction in its cytoplasm [9]. Now if the electrons used are from the metal surface, corrosion proceeds because this liberates metal ions (e.g., Fe^{2+}), hence an anodic reaction. Whereas SRB becomes a biological cathode. The presence of bacteria types that can directly take up electrons from the metal surface in a biofilm makes the biofilm electroactive [34]. This also means that the bacterium that can consume electrons must have a conductive medium for electron transfer. For a bacterium to directly consume an electron, it requires special protein membranes called pilis or

nanowires [35]. This ability of bacteria to pick up electrons directly is known as the direct electron transfer mechanism (DET) [36, 37].

Sometimes bacteria (including SRB) can consume electrons via an intermediary process, i.e., through electron mediators and by consuming reduced chemical species termed as electron careers. We refer the reader to these sources for further details about electron transport phenomena in bacteria [38-40]. The electron consumption mechanism by SRB is one major way in which MIC occurs. Below is the electrochemical representation of the BCSR mechanism [9];

$Fe \rightarrow Fe^{2+} + 2e^-$ (Metal ion Oxidation / Electron source) (4.5)

$SO_4^{2-} + 9H^+ + 8e^- \rightarrow HS^- + 4H_2O$ (Sulfate reduction / SRB Metabolism) (4.6)

From the above sulfate reaction, Bisulfide (HS^-) is a by-product of SRB metabolism. Assuming protons (H^+) are present within the environment, H_2S can be produced from the reaction below:

$HS^- + H^+ \rightarrow H_2S$ (Hydrogen sulfide formation) (4.7)

H_2S is an unpleasant compound in process facilities because it is corrosive. This H_2S formation is a simple illustration of how the metabolic by-products of a bacterium can indirectly cause corrosion. APB, however, provide a more profound mechanism of indirectly causing corrosion due to metabolism.

4.2.2.2 Acid Producing Bacteria (APB) metabolism and influence on corrosion

APB can produce metabolites such as acetic acids which can decrease the pH at the biofilm-metal interface. They can promote corrosion by accepting electrons from the metal. Also, acetic acid can contribute to corrosion by dissociating to produce hydrogen ions (H^+), which is an electron acceptor [11]. This mechanism by APB is an indirect influence on corrosion because it is not the bacteria itself that is consuming the electrons but rather its metabolites (i.e., acetic acid). Below is an electrochemical representation of APB influence on corrosion [4];

$2HAc + 2e^- \rightarrow 2Ac^- + H_2$ (direct acetic acid reduction) (4.8)

$HAc \rightarrow 2Ac^- + H^+$ (acetic acid dissociation) (4.9)

$H^+ + 2e^- \rightarrow H_2$ (proton reduction) (4.10)

Additionally, we attempt to show a synergistic process between APB and SRB that can cause corrosion in MIC. The synergy between bacteria contributes to the complexity of MIC, thus making it difficult to track which bacteria or mechanism is influencing the corrosion. Assuming we have both APB and SRB in the biofilm actively metabolizing, HS^- produced by SRB may react with the H^+ produced by acetic acid dissociation. This leads to the production of more H_2S which can also accept electrons from metal in the form of H_2S reduction [41];

$H_2S + 2e^- \rightarrow H_2 + 2HS^-$ (H_2S reduction reaction) (4.11)

4.2.2.3 Methanogens metabolism and influence on Corrosion

Methanogens require a carbon source (CO_2, H_2CO_3, HCO_3^-) as nutrients for its metabolism. They produce methane as a by-product of metabolism. However, they can cause corrosion by using electrons from the metal to reduce some of their carbon source nutrients. For example, bicarbonates (HCO_3^-) formed through dissolved CO_2 reaction processes in the presence of water, can be reduced by methanogens using electrons from the metal surface during its metabolic process [42].

Methanogenic archaea have been associated with most pitting corrosion cases and are also observed to be abundant in anaerobic environments [43, 44]. Methanogens can also affect corrosion by consuming reduced chemical species such as (H_2) [45]. These reduced chemical species can be described as electron carriers assuming they are reduced by electrons from the metal surface a priori and then later consumed by methanogens. Hence, they become electron careers for methanogens during its metabolic process. This phenomenon is known as cathodic depolarization [46]. Equation (4.12) is a chemical equation showing H_2 acting as an electron donor for HCO^-_3 reduction;

$$HCO^-_3 + 9H^+ + 8e^- \rightarrow CH_4 + 3H_2O \text{ (Bicarbonate reduction)} \quad (4.12)$$

4.2.2.4 Iron-Oxidizing Bacteria (IOB) metabolism and influence on corrosion

IOB is active in aerobic conditions. They oxidize Fe^{2+} to Fe^{3+} for energy, but the production of Fe^{3+} can lead to the formation of deposits on a metal surface [1, 47]. The deposits formed on the metal surface can induce an anodic and cathodic site adjacent to each other. This phenomenon is known as differential aeration cells [48, 49].

$Fe^{2+} \rightarrow Fe^{3+} + e^-$ (Iron (II) to Iron (III) oxidation) (4.13)

The formation of differential aeration cells is common in aerobic environments and causes corrosion when oxygen concentration at the exposed metal surface becomes the cathode, and the surface covered by precipitates becomes the anode. This can cause pitting corrosion underneath the deposits [50]. Also, surfaces under the deposits can create an anaerobic environment for the growth of SRBs and other anaerobes [51].

4.2.4 Effects of operating and environmental conditions on microbiological metabolism

Certain conditions (environmental and operating) are ubiquitous in most pipeline facility. These conditions include; temperature, flow velocity, fluid pH, pressure, flow type, dissolved CO_2 concentration, sulfide concentration. Some of these conditions have a direct influence on corrosion and bacteria activity. Here we discuss their effect on bacteria activity (metabolism) and MIC. Table 4.2 [1, 42] provides a summary of the suitable conditions necessary for bacterial metabolism. Hereon, factors, and conditions will be used interchangeably.

A suitable temperature range is necessary for optimal bacteria metabolism. The common bacteria associated with MIC are mesophilic; that means they thrive optimally between 293.15-318.15 K. pH is also a critical factor in determining metabolism because it is the measures the acidity in an environment and some of the bacteria cannot survive within certain ranges [42].

Table 4.2 Optimal conditions under which the bacteria types common to MIC metabolize.

Bacteria Group (metabolism)	Species	Temperature (K)	pH range	Nutrients	Metabolic by-product
SRB (Anaerobic)	*Desulfo-vibrio*	298.15-333.15	4-9.5	Sulfate (SO_4^{2-}), aromatic compounds lactate and acetate, hydrocarbons, organic compounds, H_2, alcohols, sulfide, and thiosulfate ($S_2O_3^{2-}$)	FeS, HS^-, H_2S
Methanogens (Anaerobic)	*Methermicoccus*	310.15-358.15	5-6	Organic compounds, CO_2 (or soluble CO_3^{2-}, HCO_3^-, H_2CO_3) or H_2	Methane (CH_4), CO
APB (Facultative)	*Clostridium aceticum*	283.15 – 313.15	Less than 7	Hydrocarbons, Organic compounds, O_2	Acetic acid (CH_3COOH), CO_2, formic acid (HCOOH)
IOB (Aerobic)	*Acidithiobacillus ferroxidans*	283.15-313.15	1-7	Ferrous iron (Fe^{2+})	Ferric iron (Fe^{3+})

4.3 Proposed Modeling Approach

In modeling complex systems that have multi-state dependencies and interactions, a Bayesian network (BN) serves as a useful tool to represent these characteristics of the system in a clear and compact graphical form. BN also provides flexibility in updating and

tracing the dependencies within the system. In this section, we describe what a BN is and why it will be useful for our modeling approach.

4.3.1 Bayesian networks (BN)

A BN is a graphical model that computes the probability of an event given some observations [14]. It is a directed acyclic graph that shows a cause-effect relationship between random variables. The graph constitutes nodes and arcs [15, 16]. The nodes are used to represent the random variables in the domain of the problem. The arcs are used to demonstrate the cause-effect relationship [15].

Each node can have either discrete finite states or continuous states. Conditional Probability Tables (CPTs) are used to quantify the probabilities of the cause-effect relationship between the states of nodes. In this work, we focus on discrete states. An example of a CPT showing the states of the simple network is given as;

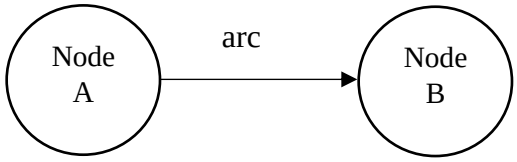

Figure 4.2 A Bayesian network of two nodes

Table 4.3 Marginal probabilities of node A with three states.

Node A		
State 1	A1	0.4
State 2	A2	0.2
State 3	A3	0.4

Table 4.4 Marginal probabilities of node B with two states.

Node B		
State 1	B1	0.65
State 2	B2	0.35

Table 4.5 CPT of the Bayesian network in Figure 4.2

Conditional Probability Table			
Node A / Node B	A1	A2	A3
B1	0.25	0.8	0.35
B2	0.75	0.2	0.65

What this CPT means is that for a given state of node A, the states in node B have a probability distribution over that given state of node A. From the table, the sum of the probabilities of states B1 and B2 over a given state A, say A1, is equal to 1. The probabilities used to fill a CPT are called Prior probabilities. They can be obtained from data in the domain that is being studied or from expert judgment. These prior probabilities are used to calculate posterior probabilities.

The posterior probability of a BN is computed based on Bayes' theorem shown in equation (4.14).

$$P(B|A) = \frac{P(A|B) \times P(B)}{P(A)} \tag{4.14}$$

The right-hand side of equation 4.14 are parameters of prior probabilities. Bayes' theorem is useful in updating a BN because it allows the input of new prior probabilities when new observations are made [52].

Practical applications of a BN involve a large network normally denoted as G, whose nodes represent random variables X_1, …., X_n. Each node X_i has a CPT that denotes dependence on its parents in the network G. Hence, the BN represents a joint distribution of the random variables via a chain rule shown in Equation (4.15) [14].

$$P(X_{1:N}) = \prod_{i=1}^{N} P(X_i|Par_G(X_i) \tag{4.15}$$

A BN can be updated by modifying the prior probabilities or adding new nodes if new observations or pieces of evidence are gathered within the domain of study. This makes the BN approach flexible and subject to improvement.

4.3.2 Model Concept

A MIC environment within a pipeline system is mostly made up of the fluid phase, which contains planktonic bacteria mixed with the fluid being transported by the pipeline, as shown in Figure 4.1. Also, a biofilm is attached to the surface of the pipe itself. Since this work considers internal corrosion, fluid flow properties will influence biofilm attachment

and formation. The surface area of the attached biofilm is usually where the corrosion site is found in the pipeline. Both anodic and cathodic sites can be under the biofilm. In Figure 4.3, the model is conceptualized under three main categories, which include: 1) Fluid and operating conditions, 2) Biofilm and bacteria metabolism and; 3) Metal surface and MIC propagation.

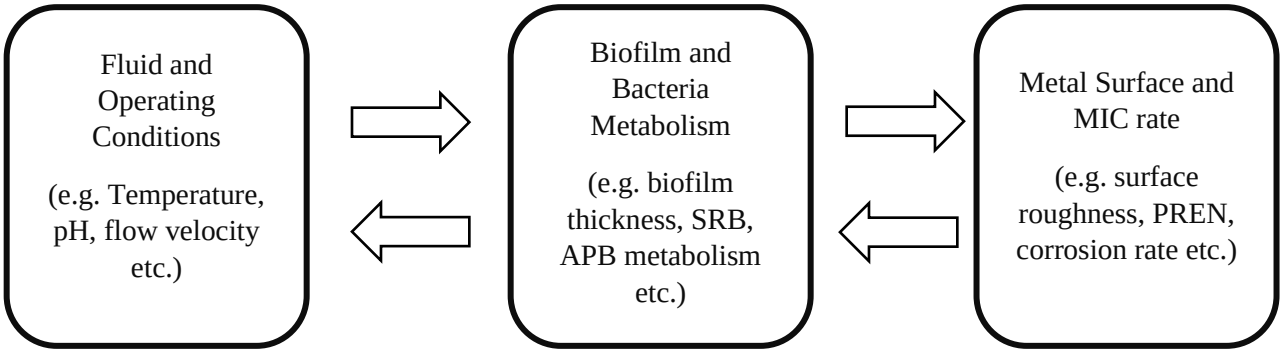

Figure 4.3 A concept of how mechanisms and factors in a MIC environment influence each other.

The arrows in Figure 4.3 show the direction of influence. For example, the temperature within the fluid phase affects the SRB, who are active within a specific temperature range. If the temperature is optimal for SRB, they can metabolize. If SRB does metabolize by sourcing energy (electrons) from the metal surface, this leads to corrosion, and thus we can determine the corrosion rate. Conversely, if the surface roughness is optimal for bacteria attachment, planktonic bacteria can settle on the metal surface leading to biofouling. Once a biofilm is formed, the metabolism of bacteria within the biofilm consortium can occur, leading to corrosion again. Also, metabolites produced by these newly attached bacteria can alter the pH in the fluid. The concept of establishing the dependencies amongst various

factors and cause-effect relation can allow us to use a BN develop a predictive model, and to perform both causal and inferential reasoning during analysis.

4.3.3 Methodology

Mitigating MIC can be difficult and complicated because the mitigation approach will require a lot of factors and mechanisms to be considered, and this approach can neither be efficient nor effective. Even though mechanistic models aim at reducing these factors when used as predictive models, this method does not provide a thorough analysis of which mechanism or operating condition correlates with or influence the corrosion rate predicted. Also, too much simplification may lead to overprediction, which has been inherent in the results of most mechanistic models published.

A method used to investigate MIC should be able to consider factors many enough to provide a thorough analysis and still provide realistic results. Therefore, a method of meeting these requirements will allow practitioners to clearly identify the most critical factors or mechanisms influencing the corrosion rate predicted by the model. A BN provides a robust framework for this requirement. The methodology proposed here is stated in five steps:

Step 1: Collect data on operating conditions and evidence of corrosion within the facility to be investigated.

Step 2: Identify bacteria types present in the biofilm consortium. This can be done using microbiologically molecular methods (MMM).

Step 3: Construct a BN based on the field data gathered and the bacteria types identified. Set the corrosion rate node as the target node.

Step 4: Set evidence in the network based on data gathered from the system under study, and then simulate the model. The key output here is to obtain the posterior probabilities of the parameters in the corrosion rate node.

Step 5: Analyze the results using sensitivity and importance analysis. This will help identify the factors in the network that are critical to the corrosion rate predicted. Consequently, these factors can be prioritized during MIC mitigation.

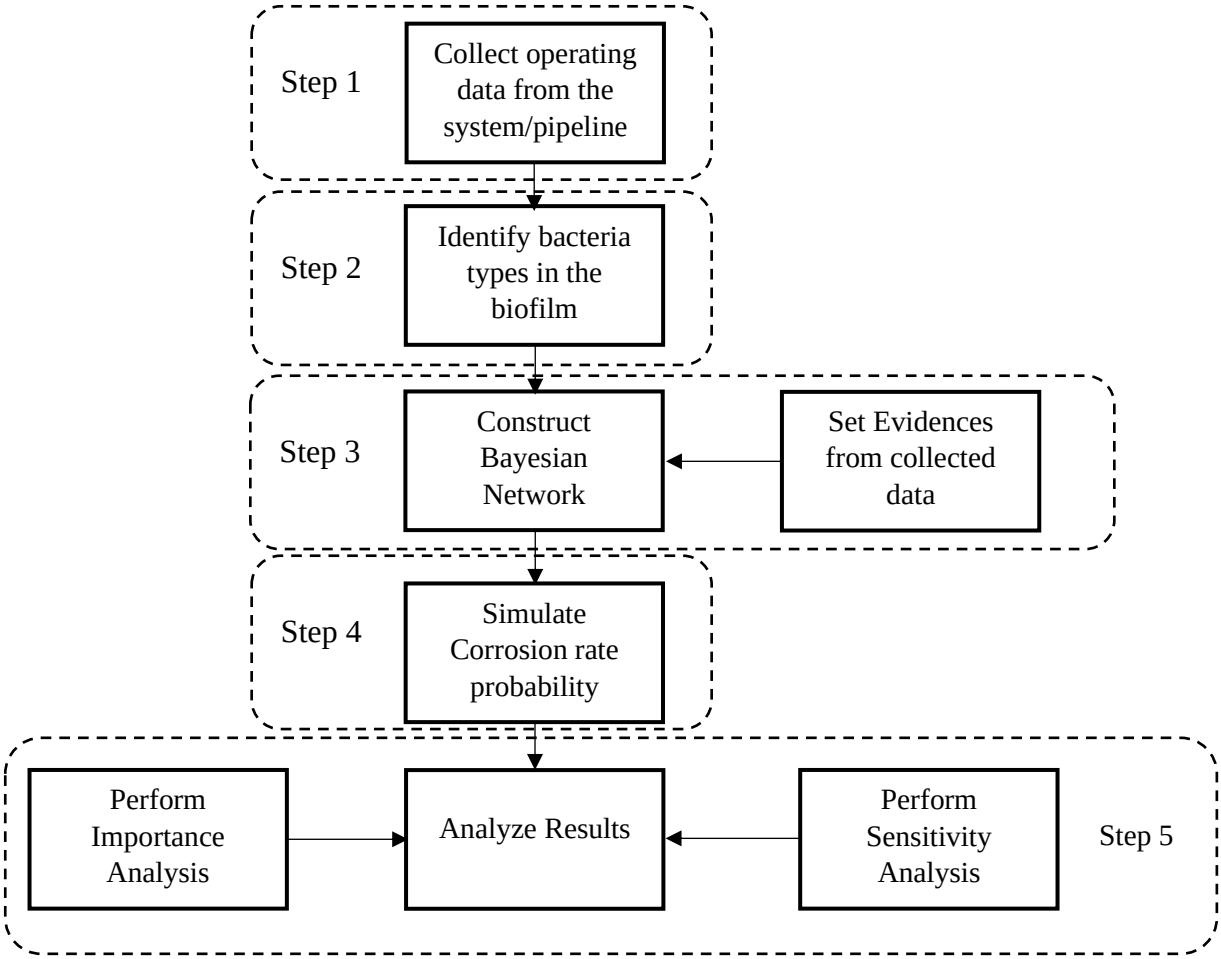

Figure 4.4 Flow diagram of the methodology

4.3.4 Domain Information and Data Collection

Investigating MIC and predicting its rate using a BN requires a definition of the nodes (i.e., factors) that makeup MIC. In the previous sections, we discussed the mechanisms and the metabolic process involved in MIC, including some common causative bacteria. The dependencies of these mechanisms have also been demonstrated. Here, we have organized the major mechanisms in MIC, including the mechanisms discussed earlier into Tables 4.6, 4.7, and 4.8. Tables 4.6, 4.7, and 4.8 represents the nodes under the categories: 1) Fluid and operating conditions, 2) Biofilm and bacteria metabolism and; 3) Metal surface and MIC propagation, respectively. Tables 4.6, 4.7, and 4.8 can be found in the appendix of this thesis.

Tables 4.6, 4.7, and 4.8 provides qualitative and quantitative information about each factor. The information about the factors is used to represent the states of each factor (node) in the network. The prior probabilities for the CPT are obtained from data used to develop mechanistic models [8, 9, 11, 26, 53], experimental works [35, 54, 55] and from critical review work on MIC mechanisms [30, 42, 49, 51, 56]. Some of the probabilities obtained from sources such as [32] include expert judgment. The works of Geno-MIC Canada research partners which include experts in MIC and microbiology like Torben Lund Skovhus (VIA University College) and Lisa Geig (University of Calgary) were critical in gathering data based on expert judgment.

4.3.5 Analysis Techniques

4.3.5.1 Importance Analysis

The domain information shows the intricate interrelation of factors involved in MIC. Once MIC rate is predicted, deciding on which factors to focus on when trying to implement mitigation techniques can be difficult because it may not be clear which of these (factors) impact the predicted corrosion rate the most. Therefore, a method is needed to enable practitioners to determine the driving factors of the corrosion rate predicted or when the corrosion rate is known. Importance analysis is a technique used to investigate the corresponding change in the observations (input factors) when the evidence in the output (predicted corrosion rate) is set to 100% [57]. The net change in probabilities (posterior) of the input variables from their previous state shows the ones that are critical to the corrosion rate predicted.

$$\%\ Change = \frac{Posterior\ probility - Prior\ Probability}{Prior\ Probability} \times 100 \qquad (4.16)$$

4.3.5.2 Sensitivity Analysis (SA)

Sensitivity analysis allows us to investigate the root cause of the corrosion rate predicted. This investigation is done by calculating the change in the predicted corrosion rate (output) when the inputs (root nodes) are changed at a sequential increase over a fixed percentage. An example of a SA procedure is that input is varied from 0% to 100% over a step change of 10%. The corresponding change in the probability of the predicted corrosion rate is recorded. Genie Software is used to perform the sensitivity analysis in this work.

4.3.6 Model Application

Figure 4.5 shows the BN model developed with the Genie software application. The network consists of the factors shown in Table 4.6, 4.7, and 4.8 as nodes. The relationship between the three major conditions is established based on the dependencies between their nodes. The network can be described as a template for the fundamental mechanisms involved in MIC that can be updated to suit different scenarios. The aim of the network (model) is to find the most probable corrosion rate, given observations/evidence from a process system. Therefore, a MIC case study is used to test the model. The evidence used are observations made from the case study.

The case study is an investigation of MIC using Microbiological Molecular Methods (MMM) in a Fully Integrated Pulp and Paper Mill process system [63]. qPCR was used to identify bacteria composition in biofilms and to investigate the possibility of bacterial growth. In this work, we use observations and evidence of MIC from a hot water pipe system in the case study, to predict the most probable corrosion rate. The evidence deduced from the case study is shown in Table 4.9.

Table 4.9 Evidence from MIC case study.

Parameter (Node)	**The value set as evidence**
Operating Temperature	~60ºC - 65ºC
Surface Roughness	>33 µm
Electron Source	metal
SRB Metabolism	Optimal metabolism
Methanogen Metabolism	Optimal Metabolism
SRB (Active)	Active (Alive)
Methanogens (Active)	Active (Alive)
Water Activity	0.6 – 0.99
FeS precipitate	High

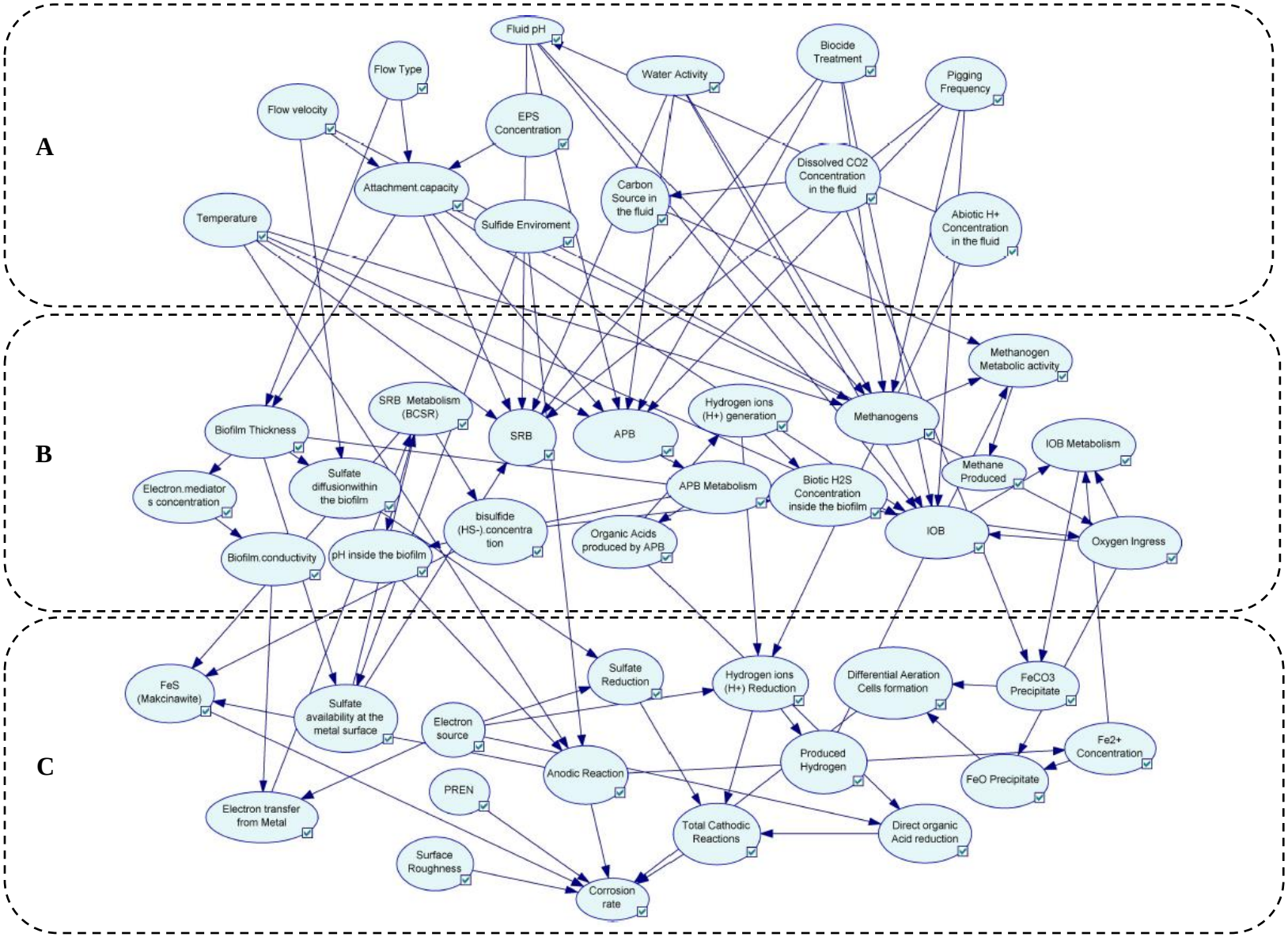
A
Fluid pH
Flow Type
Water Activity
Biocide Treatment
Pigging Frequency
Flow velocity
EPS Concentration
Attachment capacity
Carbon Source in the fluid
Dissolved CO2 Concentration in the fluid
Temperature
Sulfide Enviroment
Abiotic H+ Concentration in the fluid
B
Methanogen Metabolic activity
SRB Metabolism (BCSR)
Hydrogen ions (H+) generation
Biofilm Thickness
SRB
APB
Methanogens
IOB Metabolism
Methane Produced
Electron.mediators concentration
Sulfate diffusionwithin the biofilm
APB Metabolism
Biotic H2S Concentration inside the biofilm
bisulfide (HS-).concentration
Organic Acids produced by APB
IOB
Oxygen Ingress
Biofilm.conductivity
pH inside the biofilm
C
FeS (Makcinawite)
Sulfate Reduction
Hydrogen ions (H+) Reduction
Differential Aeration Cells formation
FeCO3 Precipitate
Sulfate availability at the metal surface
Electron source
Produced Hydrogen
Fe2+ Concentration
Anodic Reaction
FeO Precipitate
PREN
Electron transfer from Metal
Total Cathodic Reactions
Direct organic Acid reduction
Surface Roughness
Corrosion rate

Figure 4.5 BN developed from the factors and mechanisms influencing MIC. Factors are categorized under A) Fluid and operating conditions. B) Biofilm and Bacteria Metabolism C) Metal Surface and MIC propagation

From Table 4.9, surface roughness is assumed to be >33 µm because corrosion sites were at the welded parts of the piping system [63]. Because the results from the case study showed bacteria activity, we selected an optimal water activity for bacteria survival, i.e., 0.6 – 0.99. The electron source is also assumed to be from the metal due to the evidence of corrosion. Reports from the qPCR investigation showed evidence of SRB and Methanogenic growth activities. Pit depth of about 0.635 cm over a 6-year operating period was detected in the hot water piping system.

4.4 Results and Discussion

4.4.1 Corrosion Rate

After setting the evidence in the network, we calculated the posterior probabilities of the corrosion rates. Figure 4.6 is a plot of the posterior probabilities of the corrosion rate against the states in the corrosion rate node. In Figure 4.6, the model predicts 0.3 - 0.6 mm/yr. as the most probable corrosion rate based on the evidence and observations made from the hot water pipe system. By estimating the high side of 0.6 mm/yr. corrosion will result in a pit depth of 3.6 mm over six years. This prediction is quite short of the 6.35 mm pit depth reported in the case study. However, the pit depth given by the model is valid because the model considers only bacteria activities causing corrosion, which may not be the case in the hot water piping system over six years. The reason is that other forms of

corrosion which are not microbiologically influenced can coincide with MIC resulting in higher pit depths.

Nonetheless, the corrosion rate predicted is still high enough to cause leakages in a pipeline and thus pose as a risk, based on MIC alone. Additionally, the magnitude of the corrosion rate predicted is consistent with reports from some MIC experimental works [35, 55] in that, corrosion rates considering only microbiological organisms are mostly below 1 mm/yr.

We also further investigate which observation or evidence (factors) are critical to the predicted corrosion rate (output) and how sensitive the output is to the nodes of the network.

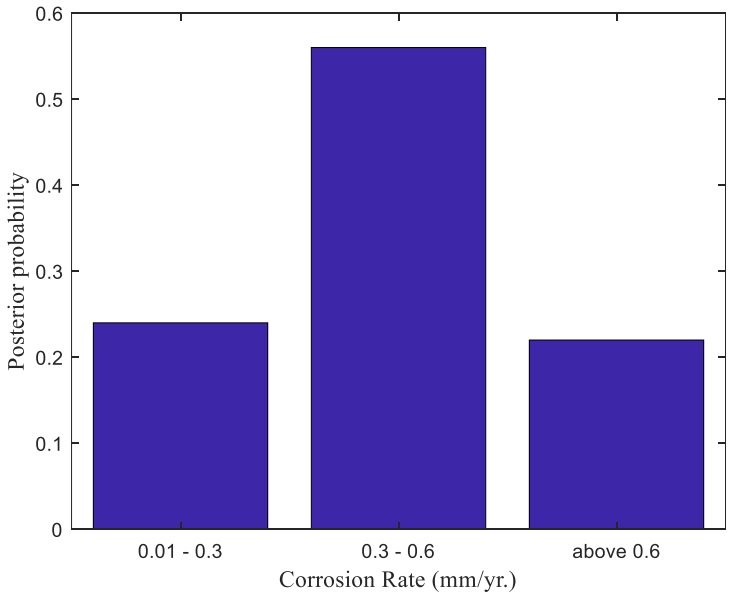

Figure 4.6 Posterior probabilities of the corrosion rate from the simulation.

4.4.2 Identifying critical nodes/factors to the output using Importance analysis

Due to the complexity of the MIC process, deciding on which factors to mitigate become overwhelming because it is not clear as to which factors are critical in driving the corrosion process. We can perform Importance analysis to identify the critical factors. This is a technique used for evidential reasoning, where the output in a BN model is used to reason about the inputs.

Here, the corrosion rate of 0.3-0.6mm/yr. is set to 100%, and the percentage change in the posterior probability of the states in each node is recorded. The interpretation of a negative or positive difference in the posterior probability of the states depends on the role of that node (factor) under study.

The results have been categorized under the three primary conditions considered in the model, i.e., 1) Fluid and operating conditions, 2) Biofilm and bacteria metabolism and; 3) Metal surface and MIC propagation in Tables 4.10, 4.11 and 4.12 respectively. This will allow us to determine the critical nodes under each major condition.

In Table 4.10, the node carbon source nutrient shows the highest variation in its states. The state high, in the carbon source nutrient node, shows a 145.28% change in its posterior probability. The result means that if there is evidence of corrosion rate being within 0.3-0.6mm/yr. this rate is highly influenced by the presence of high carbon source nutrients. Carbon is a key nutrient source for methanogen metabolism. Looking back at the mass and charge transfer mechanisms in corrosion, electrons will become a limiting factor for methanogen metabolism because the carbon source nutrients species become abundant

(i.e., High). Therefore, if electrons are taken from the metal surface via cathodic depolarization, leading to a charge transfer-controlled process. Also, because electron transfer under a charge transfer-controlled reaction is a fast process, it will result in high metabolic activity for methanogens. Table 4.11 shows the increase in metabolism for methanogen by showing a net positive change of 0.48% in high methanogen metabolic state. Since the model assumes that the bacteria are mostly sourcing energy (electrons) from the metal, Methanogens are considered a threat under this corrosion rate.

Net positive deviations in high pH and temperature states in Table 4.10 shows a negative effect on the nodes active SRB, APB, Methanogens, and IOB. The posterior probability change in the bacteria active state is reduced by 0.15%, 0.38%, 0.02% in Methanogens, SRB, and APB, respectively, in Table 4.11. However, a slight positive 0.06% change in IOB being active is observed in Table 4.11, and this could be due to their dependence on oxygen which also has 0.15% increase in the state high oxygen ingress. Also, there is a 0.71% increase in the state high IOB metabolism and a 1.25% increase in the state high differential aeration cells formation (formed due to IOB activities). The increase in the state high differential aeration cells formation is expected because IOB metabolizes to produce Fe^{3+}. Additionally, the increase in the state high oxygen ingress can result in the production of ferrous and ferric oxide deposits on the metal surface. Deposits formed on the metal surface can induce anodic and cathodic regions on the metal surface and thereby lead to corrosion.

Even though methanogens also show high metabolic rates and high methane production (+0.45%), their active states are slightly affected by the changes in environmental

conditions such as pH and temperature, unlike IOB. Hence IOB is likely to dominate this corrosion rate predicted. Furthermore, the qPCR report from the case study also showed evidence of IOB activities and growth.

Table 4.10 Percent change in posterior probability of parameters in nodes under Fluid and Operating Conditions category.

Nodes	States	% Change in Posterior probability
Temperature	298.15 – 308.15 K	-0.05
	308.15 – 333.15 K	0.01
	333.15 K – 358.15 K	0.02
Flow velocity	0-0.83 m/s	0.10
	0.83-1.6 m/s	0.02
	1.6 – 2.5 m/s	-0.05
Flow type	Stagnant	0.12
	Intermittent	-0.01
	Continuous	-0.23
Fluid pH	[1-4]	-18.77
	[4-9]	11.19
	[9-14]	11.32
EPS concentration	Low	0.04
	High	-0.01
Water activity	below 0.6	-0.04
	0.6-0.99	0.01
	above 0.99	-0.15
Pigging frequency	1-3 times/yr.	0.01
	3-6 times/yr.	-0.01
Dissolved CO2 concentration	Low	-0.15
	High	0.08
Sulfide concentration in environment	Low	-0.13
	High	0.05
Biocide treatment	0-2 times/yr.	0.00
	2-4 times/yr.	-0.01
Attachment capacity	Low	0.10

	Medium	0.04
	High	-0.09
Abiotic H^+ concentration	Low	-1.17
	High	2.17
Carbon source nutrient	Low	-66.79
	High	145.28

Table 4.11 shows the node with the highest increase being Biofilm thickness under the biofilm and bacteria metabolism category. Posterior probability changes in the states medium and high biofilm thickness increased by 21.71% and 15.43% respectively. Consequently, the state high sulfate concentration at the metal surface decreased by 0.30% in Table 4.12, and this is consistent with the concept of mass transfer limitation of nutrients by a thick biofilm. SRB depend on sulfate as a key nutrient, the low SRB metabolism state increased by 3.05% and the state high SRB metabolism decreased by 0.57% due to the mass transfer limitation posed by the increase in biofilm thickness.

In Table 4.11, however, there is an increase in high metabolism for APB, Methanogens, and IOB by 0.18%, 0.71%, and 0.48%. This means that metabolic growth APB, Methanogens, and IOB within the biofilm increases biofilm thickness and might make nutrients unavailable for SRB interfacing the metal surface. Here we assume that SRB gain electrons via DET and so they must interface the metal surface. We do not make this assumption for Methanogen, APB and IOB because for Methanogens, H_2 can shuttle electrons to them based on CDT, APB affects corrosion via its metabolic by-products and IOB causes corrosion via produced deposits forming differential aeration cells.

Even though SRB and FeS are present in the case study, the result from the model shows other bacteria types possibly limiting SRB influence in this MIC condition. This is not to say that SRB is not contributing to MIC in this case, but they may not be the dominant contributors.

Table 4.11 Percent change in posterior probability of parameters in nodes under Biofilm and Bacteria Metabolism category.

Nodes	States	% Change in Posterior probability
Biofilm thickness	Low	-19.47
	Medium	21.71
	High	15.43
Active Methanogens	Active	-0.15
	Dormant	0.17
Active SRB	Active	-0.38
	Dormant	0.52
Active APB	Active	-0.02
	Dormant	0.03
Active IOB	Active	0.06
	Dormant	-0.08
SRB metabolism	Low	3.05
	Medium	-1.15
	High	-0.57
APB metabolism	Low	0.03
	Medium	-0.39
	High	0.18
IOB metabolism	Low	-0.48
	Medium	-0.11
	High	0.71
Methanogen metabolism	Low	-0.98
	Medium	0.11
	High	0.48
Biofilm conductivity	Low	-0.002

	High	0.002
Electron mediator concentration	Low	-0.01
	High	0.01
pH inside biofilm	[1-4]	0.15
	[4-9]	0.07
	[9-14]	-0.08
Produced organic acids	Low	-0.88
	High	0.68
Oxygen ingress	Low	-0.47
	Medium	-0.07
	High	0.15
Produced methane	Low	-0.55
	Medium	0.04
	High	0.42
Biotic H_2S produced	Low	-0.25
	High	0.22
Biotic bisulfide (HS-) produced	Low	0.86
	Medium	-0.46
	High	-0.22
Sulfate diffusivity within the biofilm	Low	-2.29
	Steady	0.43
	High	0.88
Hydrogen (H^+) produced by APB	Low	-4.98
	Medium	-4.707
	High	2.95

The nodes total cathodic reactions and surface roughness show high changes, i.e. (charge-transfer controlled reaction state) 15.72% and 2.45% in Table 4.12. This is expected because cathodic reactions are required for any corrosion process to proceed. Considering the cathodic reactions that the total cathodic reaction node depends on, the charge transfer state of the nodes H^+ reduction, sulfate reduction, and organic acid reduction increased by 5.59%, 2.53%, and 3.29% respectively. Based on the nutrients available to each bacteria

type, there is an abundant carbon nutrient source for methanogens; hence, they will need electrons to proceed with metabolism. H_2 formed from reduced H^+ is a key electron donor for methanogens. The state high H^+ produced by APB is increased by 2.9%, which compounds to the high H^+ concentration in the environment. Therefore, if methanogens consume electrons via H_2 (cathodic depolarization), rapid H^+ reduction is required; hence, a charged transferred controlled reduction process is expected for H^+ reduction.

Also, the increase in high metabolism state (+0.18%) in APB means that more organic acids are likely to be produced. A high concentration of organic acid within the environment undergoing reduction reaction will be a charged transfer-controlled process. Furthermore, in Table 4.11, there is an increase in the low pH state (0.15%) in the pH inside biofilm node. However, there is an increase in the high pH state (11.32%) within the fluid (environment). The pH disparity in the biofilm and environment is consistent with the concept of ennoblement, which describes conditions within the biofilm being different from its immediate surroundings [56]. The increase in low pH state inside the biofilm is likely to be caused by APB and SRB.

To further justify that SRB may not be dominant here, in Table 4.12, sulfate reduction being controlled by charged transfer increased by 2.53% which is the lowest amongst the other charged transfer-controlled cathodic reactions, i.e., organic acid reduction (3.29%) and H^+ reduction (5.59%). Furthermore, biofilm thickness may also be limiting the sulfate reduction process due to nutrient limitation. Hence less influence of SRB on MIC in this case.

Table 4.12 Percent change in posterior probability of parameters in nodes under Metal Surface and MIC Propagation category.

Nodes	States	% Change in Posterior probability
Surface roughness	below 0.16	-19.58
	0.16 - 3.3	0.71
	above 3.3	2.45
Sulfate concentration at the metal surface	Low	0.89
	Medium	-0.11
	High	-0.30
Pitting Resistance Number (PREN)	Below 32	2.27
	32-38	-1.23
	above 38	-2.41
Anodic reaction	Charge transfer-controlled	1.32
	Mass transfer-controlled	-3.57
Total cathodic reaction	Charge transfer-controlled	15.72
	Mass transfer-controlled	-29.28
Differential aeration cells formation	Low	-1.80
	High	1.27
Fe^{2+} concentration	Low	-2.46
	Medium	0.00
	High	0.96
FeS precipitate	Low	4.38
	Medium	-3.34
	High	-0.06
FeO precipitate	Low	-1.34
	Medium	0.20
	High	0.84
FeCO3 precipitate	Low	-0.50
	Medium	0.10
	High	0.67
Organic acid reduction	Charge transfer-controlled	3.29
	Mass transfer-controlled	-5.32
Proton (H^+) reduction	Charge transfer-controlled	5.59
	Mass transfer-controlled	-10.11

Sulfate reduction	Charge transfer-controlled	2.53
	Mass transfer-controlled	-5.19
Electron source	Organic Carbon	-4.60
	Metal Surface	1.75
Rate of electron transfer from the metal surface	Low	-2.58
	High	0.91

4.4.3 Sensitivity analysis of the model's parameters

Sensitivity analysis allows one to determine how the probability of the corrosion rate predicted changes with a percentage change in the states of its parent nodes. This technique can be used for causal reasoning, where top-to-bottom approach of which input parameters (factors) are causing the output (corrosion rate) to occur.

The predicted corrosion rate is referred to as the target output. Figure 4.7 shows the parameters that the target output is most sensitive to. Figure 4.7 is a snapshot of the probabilities of the parameters varied at the full length of +/-100%. The top horizontal axis of Figure 4.7 shows the changes in the posterior probability of the target output. The color of the bar shows the direction in which the target output changes. The green color indicates a positive change, whereas the red color indicates a negative change. A positive change means a decrease in the posterior probability of the target output when the probability of an input parameter is varied. An increase in the posterior probability of the target output is undesirable, whereas a decrease in the posterior probability of the target output is desirable. Figure 4.7 shows that the state below 0.16μm in the surface roughness node is the most sensitive parameter. It shows a net positive change of 10.94% in the posterior probability of the target output if the surface roughness of the material is maintained below 0.16μm.

Conversely, we see negative changes in the parameters of the total cathodic reaction node. The state (Total Cathodic Reaction = *charge transfer-controlled* | Proton H^+ reduction = *charge transfer-controlled* | Direct Organic Acid reduction = *charge transfer-controlled* | Sulfate reduction = *charge transfer-controlled*) shows the highest net negative change of 6.73% in the posterior probability of the target output. The parameters here represent the states of a node and their corresponding probabilities.

Figure 4.7 A tornado plot of the most sensitive parameters to the corrosion rate predicted (0.3-0.6mm/yr.).

The sensitivity analysis simulation also provides values of coefficients labeled (a, b, and c) for each parameter in the list. These coefficients are used to generate a posterior probability function for the parameter (p) against the target output. The derivative of the function is the underlying measure of sensitivity. In our case, a negative derivative indicates a positive change in the posterior probability, and positive derivative means a negative change in the posterior probability of the target output.

Table 4.13 A hierarchical representation of the most sensitive parameters to the target output.

Sensitive parameters	States	Parameter (p)
1	(Surface roughness = *below 0.16µm*)	p_1
2	(Total cathodic reaction = *charge transfer-controlled* | Proton H^+ reduction = *charge transfer-controlled* | Direct organic acid reduction = *charge transfer-controlled* | Sulfate reduction = *charge transfer-controlled*)	p_2
3	(Total cathodic reaction = *charge transfer-controlled* | Proton H^+ reduction = *charge transfer-controlled* | Direct organic acid reduction = *mass transfer-controlled* | Sulfate reduction = mass *transfer-controlled*)	p_3
4	(Total cathodic reaction = *charge transfer-controlled* | Proton H^+ reduction = *mass transfer-controlled* | Direct organic acid reduction = *charge transfer-controlled* | Sulfate reduction = *charge transfer-controlled*)	p_4
5	(Electron source = *Organic Carbon Source*)	p_5
6	(Total cathodic reaction = *charge transfer-controlled* | Proton H^+ reduction = *charge transfer-controlled* | Direct organic acid reduction = *mass transfer-controlled* | Sulfate reduction = mass *transfer-controlled*)	p_6
7	(Surface roughness = above *3.3µm*)	p_7
8	(Corrosion rate = *0.3mm/yr. – 0.6mm/yr.*| Anodic reaction = *charge transfer-controlled*| Differential aeration cells formation = *High* | FeS precipitate = *High* | Surface roughness = *0.16µm-3.3 µm* | PREN = *below 32*| Total cathodic reaction = *charge transfer-controlled*	p_8

9	(Corrosion rate = *0.3mm/yr. – 0.6mm/yr.*| Anodic Reaction = *charge transfer-controlled*| Differential aeration cells formation = *High* | FeS precipitate = *High* | Surface roughness = *above 3.3 µm* | PREN = *below 32*| Total cathodic reaction = *charge transfer-controlled*	p_9
10	(Corrosion rate = *0.3mm/yr. – 0.6mm/yr.*| Anodic reaction = *charge transfer-controlled*| Differential aeration cells formation = *High* | FeS precipitate = *High* | Surface roughness = *0.16µm-3.3 µm* | PREN = *33-38*| Total cathodic reaction = *charge transfer-controlled*	p_{10}

The function for the posterior probability of the target output is given as:

$$T = \frac{(a \times p) + b}{(c \times p) + b} \tag{4.17}$$

The coefficients (a, b, and c) are calculated based on the algorithm used by Genie in simulating sensitivity. The variable T represents the posterior probability of the target output. The probability of the parameter is represented with *p*.

Figure 4.8 shows the trend in the posterior probability of the target output when the probability of the parameters (p) is varied by a 10% change in probability values. In Figure 4.8, the plots in red show the parameters that are causing an increase in the posterior probability of the target output whereas the plots in blue show the decrease in the posterior probability of the target output.

From Figure 4.8, we can see that bacteria consuming electrons from an organic carbon source (i.e., the plot T vs. $p_{(5)}$) decreases the posterior probability of the target output. The negative slope in plot T vs. $p_{(5)}$ is valid because bacteria will not have to depend on the

electrons from the metal for energy. Hence there will be no anodic dissolution of the metal due to bacteria metabolism.

The posterior probability of the target output increases with respect to the cathodic reactions in Figure 4.8. Cathodic reactions are required in for a complete electrochemical reaction. Therefore, it is expected to contribute to the increase in the posterior probability of the target output. In addition, metal surface properties such as surface roughness make the metal prone to corrosion. Plot (T vs. $p_{(1)}$) and (T vs. $p_{(7)}$) represent the target output against surface roughness at state [below 0.16 µm] and [above 3.3 µm] respectively.

Plot (T vs. $p_{(1)}$) and (T vs. $p_{(7)}$) in Figure 4.8 show a negative and positive slope, respectively in the posterior probability function of the target output. Surface roughness of less than 0.16 µm is less prone to corrosion than a surface of roughness above 3.3 µm because bacteria are more likely to settle and grow on areas where they can easily get attached to. Also, at the microscopic level, electrons on rough and edged surfaces do not bond the metal at high energy hence can easily be lost to ionized species in the environment.

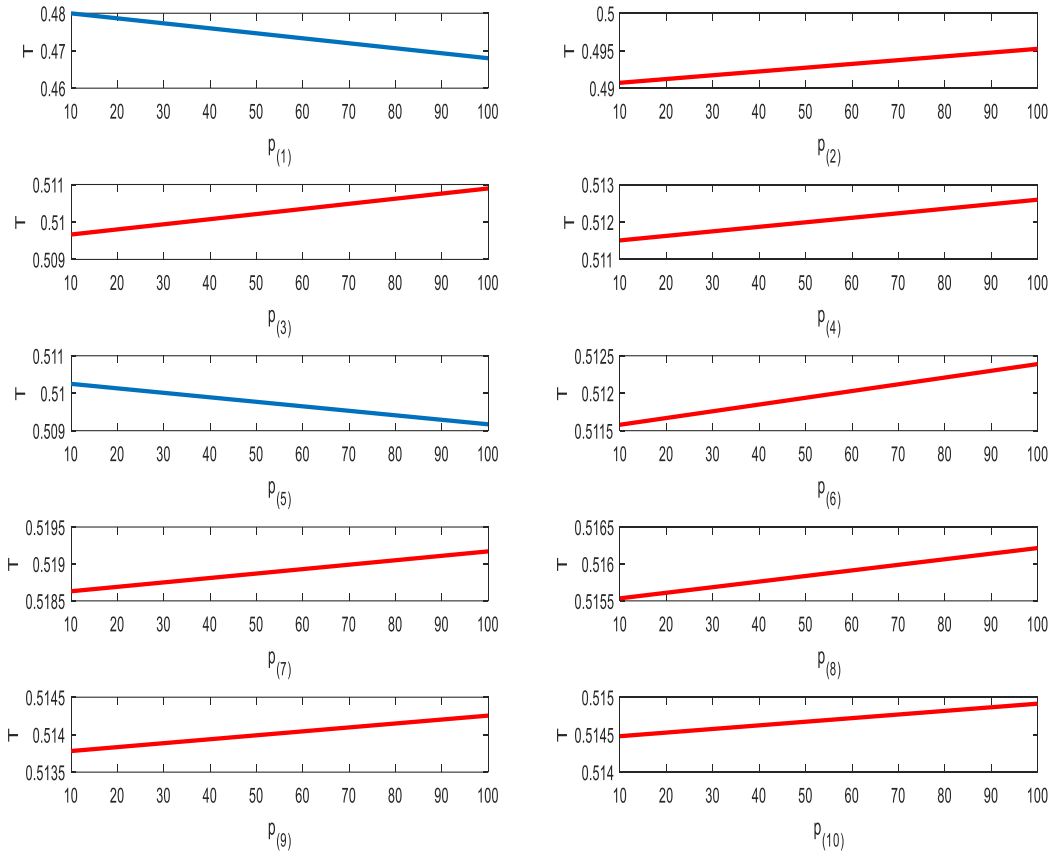

Figure 4.8 Trends in the posterior probability of the Target Output against the most sensitive parameters.

Figure 4.7 and 4.8 shows that eight out of ten of the most sensitive parameters yield negative changes. This provides a way of identifying which parameters are influencing corrosion rate predicted. Therefore, during mitigation, priority can be placed on reducing or eliminating the parameters that are positively impacting the corrosion rate predicted. Conversely, this method also shows the factors that have a negative change (i.e., reducing the posterior probability) of the predicted corrosion rate, and this information will allow operators to improve on factors that are less likely to cause corrosion. The output provided

by sensitivity analysis will enable operators to prioritize the factors to mitigate if MIC is suspected.

4.5 Conclusion

This work presents a probabilistic approach in developing a predictive model for MIC. The predictive model is developed using a Bayesian network. The network consists of 45 nodes under three major categories**;** 1) Fluid and operating conditions, 2) Biofilm and bacteria metabolism and; 3) Metal surface and MIC propagation. The interdependencies of the nodes that fall under each category are clearly illustrated using a Bayesian network. The network is fully parameterized with prior probabilities from data gathered in literature and sources that provide information based on expert judgment.

The model is tested using a MIC case study. Based on the evidence gathered from the case study and a few assumptions, the model predicts a corrosion rate ranging within 0.3-0.6mm/yr. in a hot water piping system. Analysis of the results showed a consistent relationship between microbiological metabolism, nutrients availability, and corrosion. For instance, a 0.18% increase in the high metabolism state of APB results in a 3.29% increase in charge transfer controlled reduction reaction in organic acids (APB metabolic by-products). High concentrations of organic acids (e.g., acetic acid) is expected to be produced due to increasing APB metabolism. When the concentration of the reducing species is high, the electrochemical reaction becomes a charge-transfer controlled reaction.

The analysis also shows that the corrosion rate predicted is most sensitive to the surface roughness of the material. This is true in real-life cases where rough or welded areas of a

pipeline become highly prone to corrosion. Even though the accuracy of this model is subject to the data available, its results can provide insight into a system under study. Also, practitioners can leverage the technique of Bayesian updating to incorporate more evidence and observations to improve predictions and analysis.

4.6 References

[1] B.J. Little, J.S. Lee, Microbiologically influenced corrosion, John Wiley & Sons, 2007.

[2] T.L. Skovhus, D. Enning, J.S. Lee, Microbiologically Influenced Corrosion in the Upstream Oil and Gas Industry, CRC Press, 2017.

[3] R. Javaherdashti, Microbiologically influenced corrosion: an engineering insight, Springer, 2016.

[4] T. Gu, D. Xu, Demystifying MIC mechanisms, CORROSION 2010 (2010).

[5] R. Jia, J.L. Tan, P. Jin, D.J. Blackwood, D. Xu, T. Gu, Effects of biogenic H2S on the microbiologically influenced corrosion of C1018 carbon steel by sulfate reducing Desulfovibrio vulgaris biofilm, Corros. Sci. 130 (2018) 1-11.

[6] S. Al-Jaroudi, A. Ul-Hamid, M. Al-Gahtani, Failure of crude oil pipeline due to microbiologically induced corrosion, Corrosion Engineering, Science, and Technology. 46 (2011) 568-579.

[7] W.P. Iverson, Biological corrosion, in: Advances in corrosion science and technology, Springer, 1972, pp. 1-42.

[8] A. Marciales, Y. Peralta, T. Haile, T. Crosby, J. Wolodko, Mechanistic Microbiologically Influenced Corrosion Modeling—A Review, Corros. Sci. (2018).

[9] . T. Gu, K. Zhao, S. Nesic, A New Mechanistic Model for Mic Based on A Biocatalytic Cathodic Sulfate Reduction Theory, NACE - International Corrosion Conference Series (2009).

[10] . T. Gu, Can acid producing bacteria be responsible for very fast MIC pitting?, NACE - International Corrosion Conference Series. 2 (2012) 1481-1493.

[11] D. Xu, Y. Li, T. Gu, Mechanistic modeling of biocorrosion caused by biofilms of sulfate reducing bacteria and acid producing bacteria, Bioelectrochemistry. 110 (2016) 52-58.

[12] M. Al-Darbi, K. Agha, M. Islam, Comprehensive modeling of the pitting biocorrosion of steel, The Canadian Journal of Chemical Engineering. 83 (2005) 872-881.

[13] C. Peng, S. Suen, J. Park, Modeling of anaerobic corrosion influenced by sulfate-reducing bacteria, Water Environ. Res. 66 (1994) 707-715.

[14] D. Koller, N. Friedman, F. Bach, Probabilistic graphical models: principles and techniques, MIT press, 2009.

[15] R.E. Neapolitan, Learning bayesian networks, Pearson Prentice Hall Upper Saddle River, NJ, 2004.

[16] F.V. Jensen, An introduction to Bayesian networks, UCL press London, 1996.

[17] M.T. Amin, F. Khan, S. Imtiaz, Fault detection, and pathway analysis using a dynamic Bayesian network, Chemical Engineering Science. 195 (2019) 777-790.

[18] F. Ayello, S. Jain, N. Sridhar, G. Koch, Quantitive Assessment of Corrosion Probability—A Bayesian Network Approach, Corrosion. 70 (2014) 1128-1147.

[19] E. Castillo, J.M. Menéndez, S. Sánchez-Cambronero, Predicting traffic flow using Bayesian networks, Transportation Research Part B: Methodological. 42 (2008) 482-509.

[20] O. Shabarchin, S. Tesfamariam, Internal corrosion hazard assessment of oil & gas pipelines using Bayesian belief network model, J Loss Prev Process Ind. 40 (2016) 479-495.

[21] R. Jansen, H. Yu, D. Greenbaum, Y. Kluger, N.J. Krogan, S. Chung, A. Emili, M. Snyder, J.F. Greenblatt, M. Gerstein, A Bayesian networks approach for predicting protein-protein interactions from genomic data, Science. 302 (2003) 449-453.

[22] E. McCafferty, Introduction to corrosion science, Springer Science & Business Media, 2010.

[23] R.W. Revie, Corrosion, and corrosion control: an introduction to corrosion science and engineering, John Wiley & Sons, 2008.

[24] N. Perez, Electrochemistry and corrosion science, Springer, 2004.

[25] P. Marcus, Corrosion mechanisms in theory and practice, CRC press, 2011.

[26] T. Gu, Theoretical Modeling of the Possibility of Acid Producing Bacteria Causing Fast Pitting Biocorrosion, Journal of Microbial and Biochemical Technology. 6 (2014) 68-74.

[27] A.J. Bard, L.R. Faulkner, J. Leddy, C.G. Zoski, Electrochemical methods: fundamentals and applications, wiley New York, 1980.

[28] V.S. Bagotsky, Fundamentals of electrochemistry, John Wiley & Sons, 2005.

[29] F. Song, A comprehensive model for predicting CO2 corrosion rate in oil and gas production and transportation systems, Electrochim. Acta. 55 (2010) 689-700.

[30] R. Melchers, Mathematical modeling of the diffusion controlled phase in marine immersion corrosion of mild steel, Corros. Sci. 45 (2003) 923-940.

[31] R. Kane, Corrosion in petroleum production operations, Metals Handbook. 13 (2006) 922-966.

[32] M. Taleb-Berrouane, F. Khan, K. Hawboldt, R. Eckert, T.L. Skovhus, Model for microbiologically influenced corrosion potential assessment for the oil and gas industry, Corrosion Engineering, Science and Technology (2018) 1-15.

[33] B.J. Little, J.S. Lee, Microbiologically influenced corrosion: An update, International Materials Reviews. 59 (2014) 384-393.

[34] R. Renslow, J. Babauta, A. Kuprat, J. Schenk, C. Ivory, J. Fredrickson, H. Beyenal, Modeling biofilms with dual extracellular electron transfer mechanisms, Physical Chemistry Chemical Physics. 15 (2013) 19262-19283.

[35] H. Venzlaff, D. Enning, J. Srinivasan, K.J.J. Mayrhofer, A.W. Hassel, F. Widdel, M. Stratmann, Accelerated cathodic reaction in microbial corrosion of iron due to direct electron uptake by sulfate-reducing bacteria, Corros. Sci. 66 (2013) 88-96.

[36] T. Gu, New understandings of biocorrosion mechanisms and their classifications, Journal of Microbial and Biochemical Technology. 4 (2012) iii-vi.

[37] Y.A. Gorby, S. Yanina, J.S. McLean, K.M. Rosso, D. Moyles, A. Dohnalkova, T.J. Beveridge, I.S. Chang, B.H. Kim, K.S. Kim, D.E. Culley, S.B. Reed, M.F. Romine, D.A. Saffarini, E.A. Hill, L. Shi, D.A. Elias, D.W. Kennedy, G. Pinchuk, K. Watanabe, S. Ishii, B. Logan, K.H. Nealson, J.K. Fredrickson, Electrically conductive bacterial nanowires produced by Shewanella oneidensis strain MR-1 and other microorganisms, Proc. Natl. Acad. Sci. U. S. A. 103 (2006) 11358-11363.

[38] H. Durliat, M. Barrau, M. Comtat, FAD used as a mediator in the electron transfer between platinum and several biomolecules, Journal of Electroanalytical Chemistry and Interfacial Electrochemistry. 253 (1988) 413-423.

[39] L. Huang, J.M. Regan, X. Quan, Electron transfer mechanisms, new applications, and performance of biocathode microbial fuel cells, Bioresour. Technol. 102 (2011) 316-323.

[40] E. Marsili, D.B. Baron, I.D. Shikhare, D. Coursolle, J.A. Gralnick, D.R. Bond, Shewanella secretes flavins that mediate extracellular electron transfer, Proc. Natl. Acad. Sci. U. S. A. 105 (2008) 3968-3973.

[41] T. Liengen, R. Basseguy, D. Feron, I. Beech, V. Birrien, Understanding biocorrosion: fundamentals and applications, Elsevier, 2014.

[42] A. Ibrahim, K. Hawboldt, C. Bottaro, F. Khan, Review and analysis of microbiologically influenced corrosion: the chemical environment in oil and gas facilities, Corrosion Engineering, Science, and Technology. 53 (2018) 549-563.

[43] K. Usher, A. Kaksonen, I. MacLeod, Marine rust tubercles harbour iron corroding archaea and sulfate reducing bacteria, Corros. Sci. 83 (2014) 189-197.

[44] . J. Larsen, K. Rasmussen, H. Pedersen, K. Sørensen, T. Lundgaard, T.L. Skovhus, Consortia of MIC bacteria and archaea, causing pitting corrosion in top side oil production facilities (2010).

[45] R. Boopathy, L. Daniels, Effect of pH on Anaerobic Mild Steel Corrosion by Methanogenic Bacteria, Appl. Environ. Microbiol. 57 (1991) 2104-2108.

[46] L. Daniels, N. Belay, B.S. Rajagopal, P.J. Weimer, Bacterial Methanogenesis and Growth from CO2 with Elemental Iron as the Sole Source of Electrons, Science. 237 (1987) 509-511.

[47] . D. Starosvetsky, R. Armon, J. Yahalom, J. Starosvetsky, Pitting corrosion of carbon steel caused by iron bacteria, International Biodeterioration & Biodegradation. 47 (2001) 79-87. https://doi.org/10.1016/S0964-8305(99)00081-5.

[48] T. Rao, T. Sairam, B. Viswanathan, K. Nair, Carbon steel corrosion by iron oxidising and sulfate reducing bacteria in a freshwater cooling system, Corros. Sci. 42 (2000) 1417-1431.

[49] . H.A. Videla, L.K. Herrera, Chapter 7 Biocorrosion, Studies in Surface Science and Catalysis. 151 (2004) 193-218. https://doi.org/10.1016/S0167-2991(04)80148-4.

[50] H. Flemming, P.S. Murthy, R. Venkatesan, K. Cooksey, Marine and industrial biofouling, Springer, 2009.

[51] K.M. Usher, A.H. Kaksonen, I. Cole, D. Marney, Critical review: Microbially influenced corrosion of buried carbon steel pipes, International Biodeterioration, and Biodegradation. 93 (2014) 84-106.

[52] Y. Yang, F. Khan, P. Thodi, R. Abbassi, Corrosion induced failure analysis of subsea pipelines, Reliab. Eng. Syst. Saf. 159 (2017) 214-222.

[53] J. Velazquez, F. Caleyo, A. Valor, J. Hallen, Predictive model for pitting corrosion in buried oil and gas pipelines, Corrosion. 65 (2009) 332-342.

[54] R. Avci, B. Davis, M. Wolfenden, I. Beech, K. Lucas, D. Paul, Mechanism of MnS-mediated pit initiation and propagation in carbon steel in an anaerobic sulfidogenic media, Corros. Sci. 76 (2013) 267-274.

[55] D. Xu, Y. Li, F. Song, T. Gu, Laboratory investigation of microbiologically influenced corrosion of C1018 carbon steel by nitrate-reducing bacterium Bacillus licheniformis, Corros. Sci. 77 (2013) 385-390.

[56] B.J. Little, J.S. Lee, R.I. Ray, The influence of marine biofilms on corrosion: a concise review, Electrochim. Acta. 54 (2008) 2-7.

[57] M.T. Amin, F. Khan, S. Imtiaz, Dynamic availability assessment of safety-critical systems using a dynamic Bayesian network, Reliab. Eng. Syst. Saf. 178 (2018) 108-117.

[58] B. Korth, L.F. Rosa, F. Harnisch, C. Picioreanu, A framework for modeling electroactive microbial biofilms performing direct electron transfer, Bioelectrochemistry. 106 (2015) 194-206.

[59] H. Li, D. Xu, Y. Li, H. Feng, Z. Liu, X. Li, T. Gu, K. Yang, Extracellular electron transfer is a bottleneck in the microbiologically influenced corrosion of C1018 Carbon steel by the biofilm of sulfate-reducing bacterium Desulfovibrio vulgaris, PLoS ONE. 10 (2015).

[60] G. Reguera, K.P. Nevin, J.S. Nicoll, S.F. Covalla, T.L. Woodard, D.R. Lovley, Biofilm and nanowire production leads to increased current in Geobacter sulfurreducens fuel cells, Appl. Environ. Microbiol. 72 (2006) 7345-7348.

[61] C.I. Torres, A.K. Marcus, H. Lee, P. Parameswaran, R. Krajmalnik-Brown, B.E. Rittmann, A kinetic perspective on extracellular electron transfer by anode-respiring bacteria, FEMS Microbiol. Rev. 34 (2010) 3-17.

[62] R. Jia, D. Yang, D. Xu, T. Gu, Electron transfer mediators accelerated the microbiologically influence corrosion against carbon steel by nitrate-reducing Pseudomonas aeruginosa biofilm, Bioelectrochemistry. 118 (2017) 38-46.

[63] . C. Baird, D. Ogles, B.R. Baldwin, Molecular microbiological methods to investigate microbial influenced corrosion in fully integrated kraft pulp and paper mills, NACE - International Corrosion Conference Series. 2 (2016) 1293-1303.

Chapter 5

Summary, Conclusion and Future Work Scope

5.1 Summary and Conclusion

Mitigating and controlling MIC requires a good understanding of the underlying mechanisms involved in the process. This work presents a mechanistic model and a probabilistic model which aims at predicting and mitigating MIC.

The mechanistic model studies the direct contact extracellular electron transfer process of electroactive biofilms and nutrient consumption as a controlling step in MIC. In the mechanistic model, the role of biological redox intermediaries, i.e., cytochromes embedded in the cell structure of electroactive bacteria is hypothesized as a terminal electron acceptor. The aim of the hypothesis is to compare the MIC rates when sulfate is considered the terminal electron acceptor. The mechanistic model also investigates the effect of biofilm thickness on MIC rates. The model compares the MIC rates of two biofilms of thickness 5 and 20 microns. This biofilm thickness investigation shows that when nutrient availability is considered a limiting step in MIC, a thick biofilm impedes or results in lower corrosion rate as compared to a relatively thin biofilm. This disparity in corrosion rates amongst biofilms of different thickness is due to the impact of mass transfer resistance of nutrients transported within the biofilm.

The probabilistic model developed in this work using the Bayesian network approach is based on translating and expanding the factors and mechanism considered in the mechanistic model. The probabilistic model provides the flexibility of incorporating and

analyzing many factors observed and studied in MIC. The aim of the probabilistic model is to predict the maximum corrosion rate and determine the factors that impact and are sensitive to the predicted corrosion rate. These analyses are done using Importance analysis and sensitivity analysis technique. The model was validated by applying it to a case study. The model predicted a maximum corrosion rate well within the range of the real corrosion rate data recorded in the case study. The analysis techniques used also allowed us to establish consistent theoretical expositions, such as the correlation between bacteria metabolism and corrosion. Also, the effect bacteria activities changing the chemistry in the biofilm environment compared to the bulk environment was analyzed. The analysis showed different pH levels in the biofilm compared to the bulk, and this observation is consistent with the idea of ennoblement. The analysis also showed bacteria activities synergizing and contributing to corrosion, an example being the production of H_2 from APB metabolism being a nutrient species for Methanogens. Lastly, the probabilistic approach allowed us to rank the factors that impact MIC the most in the case study. This technique of ranking the most impactful factors provides a practical approach in mitigating MIC because practitioners can prioritize which factors to focus on.

5.2 Future Scope of Work

The approach used in the mechanistic model to predict corrosion rates and pit depth propagation focuses on the direct contact extracellular electron transfer mechanism. However, this direct contact EET mechanism is one of three ways in which electrons can be transferred from a metal to bacteria. Mechanistic models can be developed by

considering other EET mechanisms such as; a) soluble electron shuttle; and b) solid conductive matrix discussed in this work.

The BCSR theory adopted in this work can be used to model other bacteria types that can utilize nutrients and inorganic electron source (i.e., from metals) for their metabolism.

The nodes in the Bayesian network used in the probabilistic model can be updated considering new mechanisms discovered in MIC. The model can also be improved by adding other bacteria types and their metabolic processes, causing MIC thereby improving its predictive reliability. A major improvement to the reliability in the prediction of the probabilistic model will be to develop a Dynamic Object-Oriented Bayesian network (DOOBN) which can be updated with monitorable parameters in each process system.

Appendix

Table 4.6 Summary of the nodes/factors considered in the fluid and operating conditions category.

Condition(s)	Factor (Node)	Influence and impact of the factor on microbiological organism and corrosion	Measure		Reference
			Specific measure. [states]	Qualitative Measure [Low/Med./High]	
Fluid and Operating Conditions	Temperature	Temperature affects microbiological activities and reaction kinetics. The range captures the optimal temperature range for the microbes considered.	[298.15 K – 308.15 K] , [308.15 K – 333.15 K] , [333.15 K – 358.15 K]	_	[42]
	Fluid pH	Affects microbiological activities and corrosion	[1-4] ,[4-9] ,[9-14]	_	[33, 42]
	Pigging frequency	This is done to clean up pipelines. It also used to reduce biofilm and bacteria growth.	[1-3 times/yr.], [3-6 time/yr.]	_	[32]
	Dissolved CO_2 concentration	Influences the availability of carbon source for microbes (e.g., methanogens)	_	X	[32, 42]
	Sulfide concentration in the environment	Sulfide concentration is required to provide the key nutrients for SRB metabolism.	_	X	[2, 4]
	Flow velocity	Affects the shearing and attachment of biofilms. MIC affected pipelines have recorded 0-0.25 m/s. Average	[0-0.83 m/s] , [0.83-1.6 m/s],	_	[2, 6, 32, 42]

		flow velocities of 0.54-1.58 m/s is reported in 322Tbpd crude transporting pipelines	[1.6 – 2.5 m/s and above]		
	Flow type	Laminar or turbulent flow can affect planktonic bacteria settlement in pipelines	[Stagnant], [Intermittent], [Continuous]	_	[3, 32]
	EPS concentration	Exopolysaccharides substances aids in biofilm attachment and protects bacteria in the biofilm.	_	X	[3, 41, 51]
	Water activity	This measures the water availability needed for bacteria growth. The measure ranges from 0 to 1. Bacteria growth is reported between 0.6 – 0.99. No bacteria growth occurs above 0.99 [pure water] because of zero nutrients.	[below 0.6] , [0.6-0.99] , [above 0.99]	_	[33]
	Biocide treatment	This is done to reduce or eliminate biofilm and bacteria growth.	[0-2 times/yr.], [2-4 times/yr.]	_	[32]
	Attachment capacity	This is a measure of the occurrence of biofouling. It is affected by flow velocity, type, EPS concentration, pigging.	_	X	[41]
	Abiotic H^+ concentration in the fluid	This measures the protons (H^+) produced by APB via acetic acid dissociation. This considers other possible H^+ production borne out bacteria activities.	_	X	[4, 10, 11]
	Carbon source nutrients in fluid	A key nutrient needed for methanogens. Dissolved CO_2 can	_	X	[42, 51]

		produce many carbon source nutrient species.			

Table 4.7 Summary of the nodes/factors considered under the biofilm and bacteria metabolism category.

Condition(s)	Factor (Node)	Influence and impact of the factor on microbiological organism and corrosion	Measure		Reference
			Specific measure. [states]	Qualitative Measure [Low/Med./High]	
Biofilm and Bacteria Metabolism	Biofilm thickness	Influences mass transport of nutrients to sessile bacteria close to the metal.	[1-16 microns], [16-32 microns], [above 32 microns]	_	[4, 9, 12]
	Active Methanogens	Influenced by conditions (e.g. temperature) needed to keep bacteria alive.	[active], [dormant]	_	[1, 2, 42]
	Active SRB	Influenced by conditions (e.g. pH) needed to keep bacteria alive.	[active], [dormant]	_	[1, 2, 42]
	Active APB	Influenced by conditions (e.g. nutrients) needed to keep bacteria alive.	[active], [dormant]	_	[1, 2, 42]
	Active IOB	Influenced by conditions (e.g. temperature) needed to keep bacteria alive.	[active], [dormant]	_	[1, 2, 42]
	SRB metabolism	Depends on conditions necessary for metabolism (e.g. nutrients and energy source) if bacteria are alive.	[slow rate], [normal rate], [rapid rate]	_	[36, 41, 50]
	APB metabolism	Depends on conditions necessary for metabolism (e.g. nutrients and energy source) if bacteria are alive.	[slow rate], [normal rate], [rapid rate]	_	[36, 41, 50]
	IOB metabolism	Depends on conditions necessary for metabolism (e.g. nutrients and energy source) if bacteria are alive.	[slow rate], [normal rate], [rapid rate]	_	[36, 41, 50]

	Methanogen metabolism	Depends on conditions necessary for metabolism (e.g. nutrients and energy source) if bacteria are alive.	[slow rate], [normal rate], [rapid rate]	_	[36, 41, 45, 50]
	Biofilm conductivity	Measures the possible electroactive nature of a biofilm	_	X	[58-61]
	Electron mediator concentration	Measures the concentration of the protein membranes in an electroactive bacterium that facilitates DET.	_	X	[58-61]
	pH inside biofilm	pH level changes within the biofilm due to microbiological metabolism	[High pH], [Medium], [Low pH]	_	[1, 2, 42]
	Organic acids produced by APB	The measure of metabolites produced by APB metabolism	_	X	[1, 2, 42]
	Oxygen ingress	Oxygen concentration present for aerobic bacteria such as IOB.	_	X	[1, 2, 42]
	Methane produced	The concentration of metabolites produced by methanogens	_	X	[1, 2, 42]
	Biotic H_2S concentration	H_2S formed due to SRB metabolism	_	X	[1, 2, 42]
	Bisulfide concentration	HS^- concentration produced by SRB	_	X	[1, 2, 42]
	Sulfate diffusivity in biofilm	Measure at which sulfate diffuses through a biofilm to sessile bacteria at the metal surface. This is affected by biofilm thickness	_	X	[1, 2, 12, 13, 42]
	(H+) produced by APB	The measure of H+ produced due to dissociation of Acetic acid produced by APB	_	X	[10, 11]

Table 4.8 Summary of the nodes/factors considered under the metal surface and MIC propagation category.

Condition(s)	Factor (Node)	Influence and impact of the factor on microbiological organism and corrosion	Measure		Reference
			Specific measure. [states]	Qualitative Measure [Low/Med./High]	
Metal Surface and MIC Propagation	Surface roughness	The measure of surface geometry and roughness that helps bacteria anchor to the surface. This also affects corrosion initiation.	[below 0.16µm], [0.16 - 3.3µm], [above 3.3µm]	_	[1, 2, 32, 42]
	PREN	This measures the resistivity of an alloy to pitting corrosion.	[below 32], [32 - 38], [above 38]	_	[1, 2, 32, 42]
	Anodic reaction	This describes and measures electron loss from metal. Charge transfer reactions lead to rapid electron loss compared to mass transfer.	[charge transfer controlled], [mass transfer controlled]	_	[1, 2, 32, 42]
	Differential aeration cells	This is a measure of anodic and cathodic sites induced by precipitates formed due to bacteria metabolisms and corrosion products.	_	X	[1, 2, 32, 42]
	FeS precipitate	A by-product of corrosion mostly associated with caused by SRB.	_	X	[1, 2, 42]
	FeO precipitate	Precipitates formed due to Fe^{2+} (from the anodic reaction) and oxygen.	_	X	[1, 2, 32, 42]
	$FeCO_3$ precipitate	The measure of precipitates formed due to Fe^{2+} and reactions with carbonates produced from dissolved CO_2.	_	X	[1, 2, 32, 42]
	Organic acid reduction	Reduction of Acetic acids produced by APB.	[charge transfer controlled], [mass	_	[2, 26, 42]

			transfer controlled]		
	Proton (H^+) reduction	Reduction of H^+ within the environment. This is a common reduction process associated with different types of corrosion, including MIC.	[charge transfer controlled], [mass transfer controlled]	_	[1, 2, 32, 42]
	Sulfate reduction	Reduction of sulfate by SRB. The BCSR theory describes this.	[charge transfer controlled], [mass transfer controlled]	_	[1, 2, 32, 42]
	Total cathodic reaction	Measures the total cathodic reactions driving the anodic reaction considered in the model	[charge transfer controlled], [mass transfer controlled]	_	[58, 61, 62]
	Electron source	The energy source needed by bacteria for metabolism	[metal source], [organic carbon energy source]	_	[35, 58]
	Electron transfer	Measures the rate at which electrons are removed from the metal if bacteria are sourcing energy from the metal. It also depends on biofilm conductivity.	_	X	[58, 61, 62]
	Corrosion rates	This the average corrosion rates reported in MIC investigations, experiments and predictions made by mechanistic models. MIC rates are mostly below 1mm/yr.	[0.01- 0.3 mm/yr.], [0.3 – 0.6 mm/yr.], [above 0.6 mm/yr.]	_	[9, 35, 36, 55]